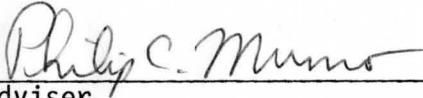
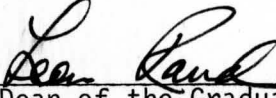


A STUDY OF MINORITY CARRIER RESPONSE
IN A METAL-INSULATOR-SEMICONDUCTOR STRUCTURE

by
Fariborz Ghoorkhanian

Submitted in Partial Fulfillment of the Requirements
for the Degree of
Master of Science in Engineering
in the
Electrical Engineering
Program


Adviser 12/20/79 Date


Dean of the Graduate School 1-3-80 Date

YOUNGSTOWN STATE UNIVERSITY

March, 1980

A STUDY OF MINORITY CARRIER RESPONSE
IN A HETEROINSULATOR-SEMICONDUCTOR STRUCTURE

Ferhuz Szorkracian
Master of Science

Youngstown State University, 1980

I would like to dedicate this thesis

to

my loving parents

The minority carrier current capacitance-voltage characteristics of MIS structures with Al_2O_3 - Ge junctions are presented.

The Poisson's and continuity equations for the semiconductor region are obtained and put into a set of first-order linear differential equations, which comprise a boundary value problem. This set of equations is solved numerically. First, the static equation in the semiconductor is solved to obtain the matrix, \mathbf{A} . Then the general method of complementary functions using the determinant method is employed. The semiconductor impedance is found and the capacitance-voltage characteristics of the MIS structures are obtained. The effect of the semiconductor sheet potential is also considered by proper changes to the boundary conditions. The charge analysis approach is also used and its results are compared to the numerical solution of state equations in different cases.

The results of this study show considerable amount of minority carrier response for Germanium-based devices even above 1 MHz. It is also found that this response depends strongly both on frequency and level of majority

ABSTRACT

A STUDY OF MINORITY CARRIER RESPONSE
IN A METAL-INSULATOR-SEMICONDUCTOR STRUCTURE

Fariborz Ghoorkhanian

Master of Science

Youngstown State University, 1980

The minority carrier effect on capacitance-voltage characteristics of MIS structures with examples for $\text{SiO}_2\text{-Si}$ and $\text{Al}_2\text{O}_3\text{-Ge}$ is studied. C-V curves for intrinsic Ge are presented.

The small-signal state equations for the semiconductor neglecting recombination are obtained and put into a set of first-order linear differential equations, $\dot{y} = Ay$, which comprise a boundary value problem. This set of equations is solved numerically. First, the static equation in the semiconductor is solved to obtain the matrix, A. Then the general method of complementary functions using the orthonormalization process is employed. The semiconductor impedance is found and the capacitance-voltage characteristics of the MIS structure are obtained. The effect of the semiconductor ohmic contact is also considered by proper changes to the boundary conditions. The charge analysis approach is also used and its results are compared to the numerical solution of state equations in different cases.

The results of this study show considerable amount of minority carrier response for Germanium-based devices even above 1 MHz. It is also found that this response depends strongly both on frequency and level of impurity.

TABLE OF CONTENTS
ACKNOWLEDGEMENTS

The author wishes to express his appreciation to his professor, Dr. Philip C. Munro, for his suggestions and support throughout the course of this work. He also wants to thank Mrs. Anna Mae Serrecchio for typing this thesis.

The author thanks God, who gave him the opportunity and time to do this work.

I	INTRODUCTION	1
II	PHYSICAL STRUCTURE	2
	Idealized Rod Structure	2
	Cross-Sections and End Regions	3
	Boundary Conditions	3
III	CHARACTER ANALYSIS	7
	Lambert's Equations	7
	Euler's Equation	8
	Low Frequency	8
	High Frequency	10
	Wave Velocity	10
IV	SMALL-SIGNAL STATE EQUATIONS	12
	Matrix Form of Equations	13
	Boundary Values	14
V	NUMERICAL SOLUTION OF SMALL-SIGNAL STATE EQUATIONS	16
	General Solution	16
	Numerical Procedure	17
	Recoupling	17

TABLE OF CONTENTS

	PAGE
ABSTRACT.	i
ACKNOWLEDGEMENTS.	ii
TABLE OF CONTENTS	iii
LIST OF FIGURES	v
LIST OF SYMBOLS	vi
CHAPTER	
I INTRODUCTION.	1
Physical Structure.	1
Idealized MIS Structure	3
Bias Regions and Band Diagrams.	3
C-V Characteristics	5
II CHARGES ANALYSIS.	7
Carrier Concentrations.	7
Poisson's Equation	8
Low Frequency	9
High Frequency.	10
Gate Voltage.	10
III SMALL-SIGNAL STATE EQUATIONS.	12
Matrix Form of Equations.	13
Boundary Values	14
IV NUMERICAL SOLUTION OF SMALL-SIGNAL STATE EQUATIONS.	16
General Solution.	16
Numerical Procedure	17
Reconditioning.	17

Application to MIS Problem.	18
Initial Vectors	19
Numerical Methods Used.	20
Method of Integration	21
Method of Orthonormalization.	22
V RESULTS	23
Convergence of the Method	24
C-V Characteristics for Al_2O_3 -Ge.	26
Effect of Ohmic Contact	33
VI SUMMARY, CONCLUSION AND SUGGESTIONS FOR FURTHER WORK.	37
Suggestions for Further Work.	38
LIST OF REFERENCES	40
APPENDIX A STATE-EQUATION PROGRAM.	42
APPENDIX B CHARGE ANALYSIS PROGRAMS.	48

LIST OF FIGURES

FIGURE	PAGE
1. Cross-Sectional View of MIS Structure.	2
2. Idealized Flat-Band Energy Diagram	2
3. Energy-Band and Charge Diagrams for Various Biases (p-Type Semiconductor)	4
4. One-Dimensional MIS Structure.	8
5. One-Dimensional MIS Structure, showing Semiconductor Impedance and Boundaries.	14
6. U versus x, showing Surface and Bulk Regions	21
7. Equivalent Circuit of the MIS Structure.	23
8. Charge Analysis versus State-Equation Approach for SiO ₂ -Si, N=14	25
9. C-V Characteristics using Charge Analysis and State-Equation Approach for Al ₂ O ₃ -Ge, p-Type	27
10. C-V Characteristics, showing Minority Carrier Response for Al ₂ O ₃ -Ge, p-Type.	28
11. C-V Characteristics, showing Effect of Doping Level for Al ₂ O ₃ -Ge, p-Type.	30
12. C-V Characteristics, showing Effect of Doping Level for Al ₂ O ₃ -Ge, n-Type.	31
13. C-V Characteristics for Al ₂ O ₃ -Ge (Intrinsic)	32
14. C-V Characteristics, showing Effect of Ohmic Contact for Al ₂ O ₃ -Ge, p-Type, U _F = 2.	34
15. C-V Characteristics, showing Effect of Ohmic Contact for Al ₂ O ₃ -Ge, p-Type, U _F = 3.	35
16. Effect of Ohmic Contact on Inversion Capacitance for R _p = R _n = .02Ω-cm ²	36

LIST OF SYMBOLS

SYMBOL	DEFINITION	UNITS OR REFERENCE
A	Gate electrode area	cm ²
C	Total capacitance of MIS	F
C _I	Insulator capacitance	F
C _S	Semiconductor capacitance	F
ε	Electric field intensity	V/cm ²
E _F	Fermi-level energy	eV or J
E _i	Intrinsic Fermi-level energy	eV or J
E ₀	Permittivity of free space	8.8542 x 10 ⁻¹⁴ F/cm
f	Frequency	Hz
F	See equation 12	
G	Conductance of MIS	mho
i	Complex number (0,1)	
J _i	Displacement current density	A/cm ²
J _n	Electron current density	A/cm ²
J _p	Hole current density	A/cm ²
K	Boltzmann constant	1.3805 x 10 ⁻²³ J/°K
K _I	Insulator relative dielectric constant	
K _S	Semiconductor relative dielectric constant	
L _D	Intrinsic Debye length	cm
n	Electron concentration	cm ⁻³
N _A	Acceptor concentration	cm ⁻³
N _D	Donor concentration	cm ⁻³
n _i	Intrinsic carrier concentration	cm ⁻³
p	Hole concentration	cm ⁻³
q	Electronic charge	1.6021 x 10 ⁻¹⁹ C

R_n	Ohmic contact resistance for electrons	$\Omega\text{-cm}^2$
R_p	Ohmic contact resistance for holes	$\Omega\text{-cm}^2$
R_s	MIS series resistance	$\Omega\text{-cm}^2$
T	Temperature	$^\circ\text{K}$
U	Normalized semiconductor potential	
U_F	Normalized semiconductor bulk Fermi potential with respect to E_i	
U_s	Normalized semiconductor surface potential	
V_G	Gate voltage	V
V_i	Electrostatic potential	V
V_n	Quasi Fermi potential for electrons	V
V_p	Quasi Fermi potential for holes	V
x_I	Insulator thickness	\AA
μ_n	Electron mobility	$\text{cm}^2/\text{V}\cdot\text{s}$
μ_p	Hole mobility	$\text{cm}^2/\text{V}\cdot\text{s}$
ξ	Normalized length	
ϕ_{ms}	Metal-to-semiconductor work-function difference	eV or J
ω	Angular frequency	s^{-1}

CHAPTER I

INTRODUCTION

The MIS (Metal-Insulator-Semiconductor) varactor is one of the most used devices in semiconductor industry. C-V (Capacitance-Voltage) characteristics of MIS have been used extensively seeking information about this structure, such as, interface surface states, fixed and mobile charges in the insulator. One of the most used devices for this purpose is SiO₂-Si. SiO₂ can be grown thermally on Silicon. The use of other semiconductors like Germanium and other kinds of insulators like Al₂O₃ have also been studied by others. [1,2,3]

Physical Structure

The MIS-C is a two terminal device composed of a thin layer of insulator sandwiched between a semiconductor substrate and a metallic field plate, Figure 1. A second metallic layer along the back side of the semiconductor serves as an ohmic contact between the semiconductor and the external circuit. This terminal is used as the reference for the applied voltage. The terminal connected to the field plate is referred to as the gate. The basic parameters of the MIS-C structure are the insulator thickness, x_I , the gate area, A , and the doping concentration in the semiconductor substrate N_A or N_D . Some typical values for a Silicon-based device are as follows: [4]

$$x_I = 1000 \text{ to } 2000 \text{ \AA}$$

$$A = (4 \text{ to } 45) \times 10^{-4} \text{ cm}^2$$

$$N_D \text{ or } N_A = 10^{14} \text{ to } 5 \times 10^{16} \text{ cm}^{-3}$$

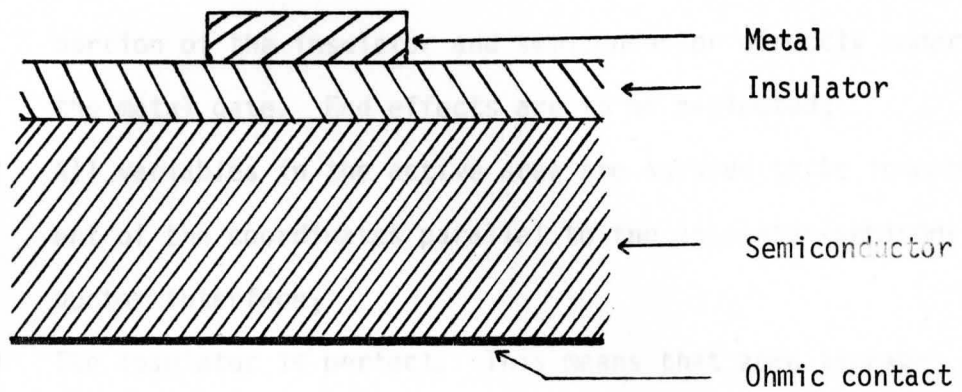


FIGURE 1. Cross-Sectional View of MIS Structure

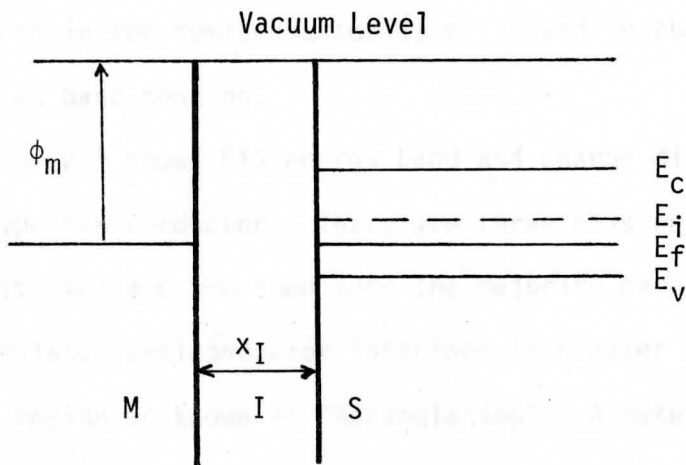


FIGURE 2. Idealized Flat-Band Energy Diagram

Idealized MIS Structure

The idealized MIS structure is to be characterized as follows:[4]

- 1) The active area of the structure is to be confined to that portion of the insulator and semiconductor directly under the metal gate. End effects are to be neglected;
- 2) All variables in the active area are assumed to be independent of the coordinates parallel to the insulator-semiconductor interface;
- 3) The insulator is perfect. This means that zero leakage current flows through it under all static bias conditions;
- 4) The metal-semiconductor work-function difference, ϕ_{ms} , is assumed to be zero, Figure 2.

Bias Regions and Band Diagrams

The voltage applied to the gate of the MIS will be dropped partly across the insulator and partly across the semiconductor. A voltage drop in the semiconductor is reflected in the energy band structure as band bending.

Figure 3 shows MIS energy band and charge distribution diagrams for a p-type semiconductor. There are three bias regions. For an applied gate voltage less than zero the majority carrier concentration at the insulator-semiconductor interface is greater than in the bulk. This bias region is known as "Accumulation". A gate voltage slightly greater than zero causes the depletion of majority carriers for a distance into the semiconductor. This bias region is called "Depletion". As gate voltage increases, there is a point at which the concentration of minority carriers is greater than the concentration of majority carriers at the insulator-semiconductor interface. This bias region is

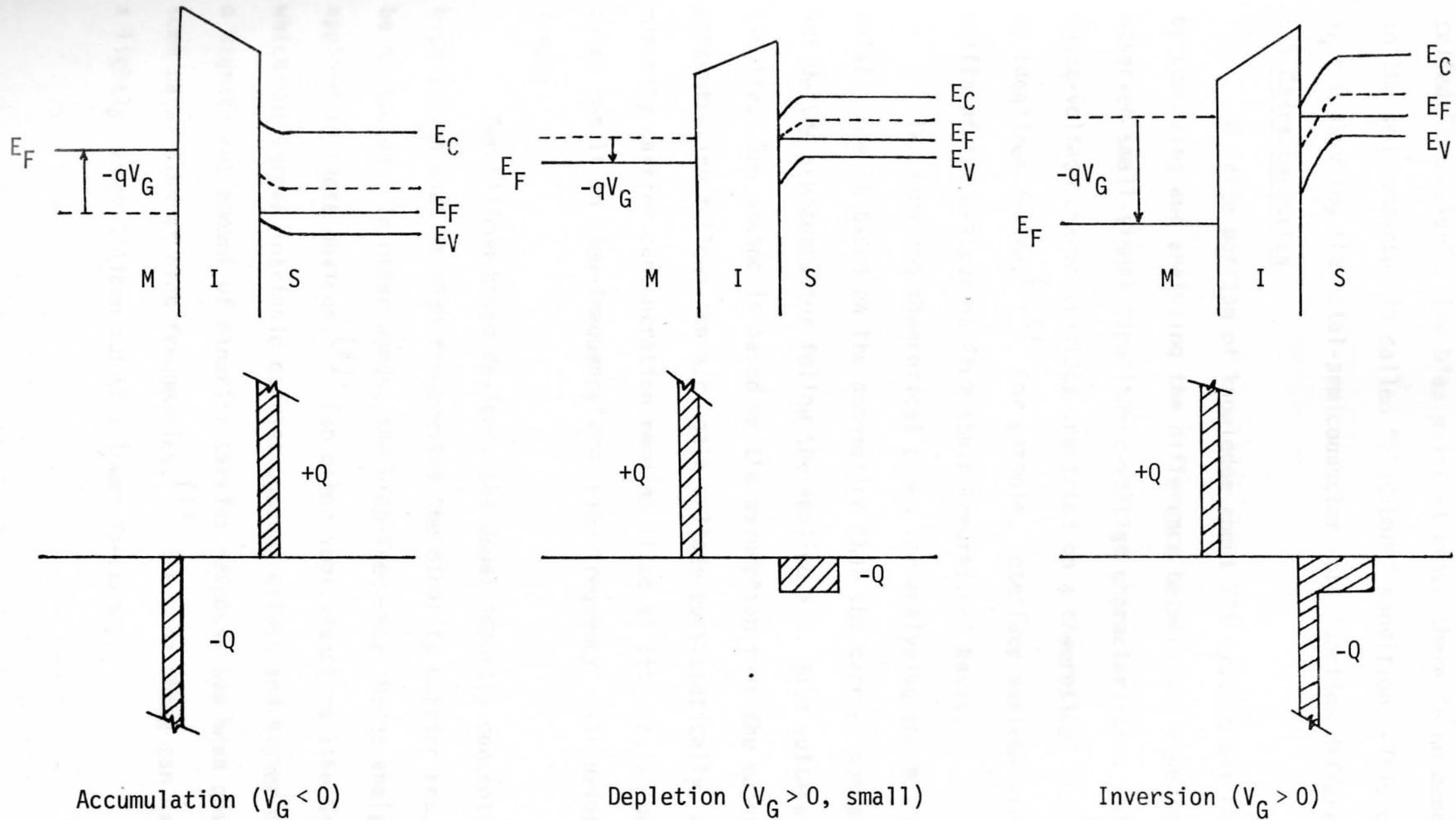


FIGURE 3. Energy-Band and Charge Diagrams for Various Biases (p-type Semiconductor)

called "Inversion". The bias point at which there is no band bending in the semiconductor is called "Flat-band" condition. This occurs at $V_G = 0$ assuming the metal-semiconductor work function difference to be zero.

C-V Characteristics

A large portion of knowledge about MIS systems has been gathered by comparing and analyzing the difference between the experimentally observed small-signal capacitance-voltage characteristics and the capacitance-voltage characteristics predicted on a theoretical basis assuming an idealized device.^[1,5] For example, interface surface states cause shifts of the C-V curves from their theoretical basis.

Two limiting theoretical cases for analyzing the MIS structures exist. One is based on the assumption that the carrier concentrations inside the semiconductor follow the applied a.c. gate voltage quasistatically. The second is based on the assumption that the majority carrier concentration follows the a.c. gate voltage quasistatically, while the minority carrier concentration remains fixed at its d.c. value. These cases result in "low-frequency" and "high-frequency" C-V curves, respectively.

For Silicon-based devices, the usual impurity concentration is high enough that at high frequencies the minority carrier response can be neglected. In other words, the high-frequency charge analysis can be applied to these devices.^[4] For other semiconductors like Germanium which have larger intrinsic carrier concentrations and higher mobilities, a significant amount of minority carrier response has been observed in some cases even at high frequencies.^[1] The same thing can happen for a lightly doped Silicon but at a lower frequency.

In this work a more complete way for analyzing the MIS structure is developed. This method includes the effect of both majority and minority carriers and their frequency response. In Chapter II a charge analysis approach to the problem is discussed. Low- and high-frequency behavior of the MIS is formulated and the semiconductor capacitance in both cases is found. In Chapter III the semiconductor behavior in small-signal excitation, which includes the effect of both carriers, is found. The obtained equations are then simplified and put into a form called "small-signal state equations".^[4] In Chapter IV a numerical method for solving the equations obtained in Chapter III is suggested. The results of using this method for MIS capacitors are discussed in Chapter V. Chapter VI summarizes the results of this work and presents suggestions for further work.

CHAPTER II

CHARGES ANALYSIS

Charge analysis is the name of an approach for establishing the low- and high-frequency C-V characteristics which requires the exact formulation of the d.c. state. In this approach, charge disturbances, resulting from the a.c. bias, and the associated capacitance are described directly in terms of the fundamental charge and voltage variables. Most of the work in this chapter follows the work of Pierret.^[4]

Carrier Concentrations

The electron and hole concentrations inside the semiconductor can be described as^[6]

$$\begin{aligned} n &= n_i \text{Exp}(-U_F) \\ p &= n_i \text{Exp}(U_F) \end{aligned} \quad (1)$$

where n_i is the intrinsic carrier concentration. U_F is a measure of doping level and is equal to $(E_i - E_F)/KT$, where E_i is the intrinsic Fermi-level energy and E_F is the Fermi-level energy.

Assuming complete ionization of impurity sites, the relation between U_F and concentration of dopants can be found by writing the neutrality equation in the semiconductor.

$$N_A - N_D = n_i (\text{Exp}(U_F) - \text{Exp}(-U_F)) \quad (2)$$

where N_A and N_D are the acceptor and donor concentrations, respectively.

Thus far, it is assumed that the piece of semiconductor is all at the same potential. An electric field inside the semiconductor causes the energy bands to shift.^[4,6] At equilibrium, the electron and hole concentrations are

$$\begin{aligned} n' &= n \text{Exp}(qV/KT) \\ p' &= p \text{Exp}(-qV/KT) \end{aligned} \quad (3)$$

where V is the electrostatic potential. Introducing a new variable called U such that, $U = qV/KT$, the above relations will be

$$\begin{aligned} n' &= n \text{ Exp}(U) \\ p' &= p \text{ Exp}(-U) \end{aligned} \quad (4)$$

Substituting from (1) for n and p , into the above equations gives

$$\begin{aligned} n &= n_i \text{ Exp}(U-U_F) \\ p &= n_i \text{ Exp}(U_F-U) \end{aligned} \quad (5)$$

Poisson's Equation

With the carrier concentrations expressed in terms of electrostatic potential, Poisson's equation can be applied to find the electric field inside the semiconductor.

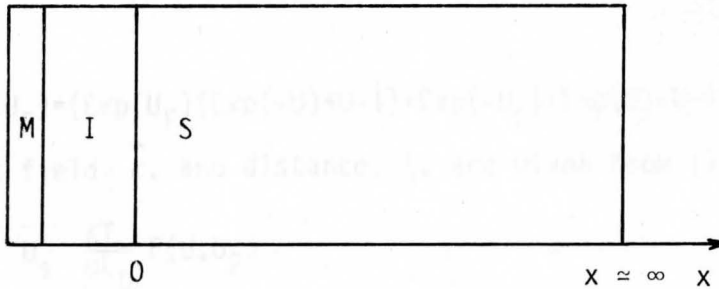


FIGURE 4. One-Dimensional MIS Structure.

Writing the Poisson's equation in a one-dimensional form

$$\frac{d^2V}{dx^2} = - \frac{\rho}{K_s \epsilon_0} \quad (6)$$

where, K_s is the semiconductor's relative dielectric constant. Defining the intrinsic Debye length, L_D , and the normalized distance, ξ , into the semiconductor as

$$L_D = \sqrt{\frac{K_s \epsilon_0 K T}{2q^2 n_i}} \quad (7)$$

and

$$\xi = \frac{x}{L_D} \quad (8)$$

the following form of Poisson's equation can be obtained

$$\frac{d^2U}{d\xi^2} = \frac{1}{2}(\text{Exp}(U-U_F) - \text{Exp}(U_F-U) + \text{Exp}(U_F) - \text{Exp}(-U_F)) \quad (9)$$

where U is a function of normalized distance, ξ .

The boundary conditions which are required to solve this electrostatic problem are taken as

$$\begin{aligned} U(0) &= U_s \\ \frac{dU}{d\xi}(\infty) &= 0 \end{aligned} \quad (10)$$

Integrating both sides of (9)

$$\frac{dU}{d\xi} = \pm F(U, U_F) \quad (11)$$

where

$$F(U, U_F) = (\text{Exp}(U_F)(\text{Exp}(-U) + U - 1) + \text{Exp}(-U_F)(\text{Exp}(U) - U - 1))^{1/2} \quad (12)$$

the electric field, $\vec{\epsilon}$, and distance, ξ , are given from (11) as

$$\vec{\epsilon} = \hat{U}_s \frac{KT}{qL_D} F(U, U_F) \quad (13)$$

and

$$\xi = -\hat{U}_s \int_{U_s}^U \frac{dU'}{F(U', U_F)} \quad (14)$$

where \hat{U}_s is the sign of U_s .

Low Frequency

In the low frequency assumption, all the carriers in the semiconductor follow the applied a.c. signal. Considering this, the corresponding semiconductor capacitance, C_s , can be formulated as [4]

$$C_s = \hat{U}_s \frac{K_s E_0}{2L_D} \frac{\text{Exp}(U_F)(1 - \text{Exp}(-U_s)) + \text{Exp}(-U_F)(\text{Exp}(U_s) - 1)}{F(U_s, U_F)} \quad (15)$$

High Frequency

In high frequency the normal assumption is that the frequency is high enough that the minority carriers can not follow the applied a.c. signal. Therefore, their concentration is fixed at the d.c. level. On the other hand, the frequency is low enough so that the majority carriers can follow the applied signal completely.

Starting with Poisson's equation, as the low-frequency case, and assuming a p-type bulk, the semiconductor capacitance can be obtained as^[4]

$$C_s = \hat{U}_s \frac{K_s E_0}{2L_D} \frac{\text{Exp}(U_F)(1-\text{Exp}(U_s))}{(\text{Exp}(U_F)(\text{Exp}(-U_s) + U_s - 1))^{1/2}} \quad U_s \leq U_F \quad (16)$$

$$C_s = \frac{K_s E_0}{L_D} \frac{1}{\int_{U_F}^{U_s} \frac{dU'}{F(U', U_F)} + \frac{2(\text{Exp}(U_F)(\text{Exp}(-U_F) + U_F - 1))^{1/2}}{\text{Exp}(U_F) - 1}} \quad U_s \geq U_F \quad (17)$$

Gate Voltage

The static solution of MIS can be completed by finding the gate voltage in terms of normalized surface potential, U_s . Using relation (13) the gate voltage can be obtained as

$$V_G = \frac{KT}{q} (U_s + \hat{U}_s \frac{K_s X_I}{L_D K_I} F(U, U_F)) \quad (18)$$

where X_I and K_I are the thickness and relative dielectric constant of the insulator, respectively.

Charge analysis is used in this work to have a basis for comparison with the method of state-equations that is found in Chapter III. Equation (18) is used to find gate voltage for a particular U_s . Equation (11) is used to produce subintervals needed for the solution of state

equations. Low- and high-frequency charge analysis computer programs are given in Appendix B.

At an intermediate frequency, when the carriers follow the applied signal partially and their effect can not be neglected, the charge analysis method, which includes the effect of minority carriers on the semiconductor capacitance, can be applied. Because of this, another line of approach to the problem is required. The effect of both carriers is needed. This method is usually achieved by formulating the continuity equations of electrons and holes while taking the continuity and Poisson's equation in the semiconductor. These equations in their initial form are very complex and cannot be solved easily. In the case of MIS-C system some assumptions apply that lead us to a simpler set of relations. These assumptions are as follows:

- (1) The MIS system is at quasi-equilibrium. This means that electron and hole average currents are zero.
- (2) The system is excited by a small sinusoidal signal.
- (3) The recombination-generation rate of the disturbed carriers is negligible.
- (4) The gate area of MIS-C system is large enough, compared to its length, that the electric field is constant in a one-dimensional form.

After applying the above assumptions, the form of the small-signal state equations, which are also called the continuity equations [1]

will be

$$\frac{\partial n}{\partial t} + \frac{\partial J_n}{\partial x} = 0$$

$$\frac{\partial p}{\partial t} + \frac{\partial J_p}{\partial x} = 0$$

CHAPTER III
SMALL-SIGNAL STATE EQUATIONS

At an intermediate frequency, minority carriers follow the applied a.c. signal partially and their effect can not be neglected. So, the charge analysis method, which either includes or neglects the effect of minority carriers on the semiconductor capacitance, can not be used. Because of this, another line of approach to the problem which includes the effect of both carriers is needed. This method is obtained^[4,6] by formulating the conduction mechanism of electrons and holes while imposing the continuity and Poisson's equations in the semiconductor. These equations in their entire form are very complex and can not be solved easily. In the case of MIS-C system some assumptions apply that lead us to a simpler set of relation. These assumptions are as follows:

- 1) The MIS system is at quasi equilibrium. This means that electron and hole average currents are zero;
- 2) The system is excited by a small sinusoidal signal;
- 3) The recombination-generation rate of the disturbed carriers is negligible;
- 4) The gate area of MIS-C system is large enough, compared to its length, that the equations can be expressed in a one-dimensional form.

After applying the above assumptions, the form of the small-signal state equations, which are also called small-signal transport equations^[7] will be

$$J_n = - \sigma_n \frac{dV_n}{dx}$$

$$J_p = - \sigma_p \frac{dV_p}{dx}$$

$$J_i = -i\omega K_s E_0 \frac{dV_i}{dx}$$

$$i\omega c_n (V_n - V_i) + \frac{dJ_n}{dx} = 0 \quad (19)$$

$$i\omega c_p (V_p - V_i) + \frac{dJ_p}{dx} = 0$$

$$\frac{dJ_i}{dx} = i\omega c_n (V_n - V_i) + i\omega c_p (V_p - V_i)$$

where J_n and J_p are the electron and hole conduction currents and J_i is the displacement current. V_n and V_p are the quasi Fermi potentials for electrons and holes. V_i is the electrostatic potential. μ_p and μ_n are the carrier mobilities in the bulk. $K_s E_0$ is the permittivity of the semiconductor and ω is the angular frequency of the applied signal and i designates the complex number, $(0,1)$. The factors σ_n , σ_p , c_p and c_n are defined as

$$\sigma_p = q\mu_p P \quad \text{and} \quad \sigma_n = q\mu_n N$$

$$c_p = q^2 P / KT \quad \text{and} \quad c_n = q^2 N / KT \quad (20)$$

where N and P are the static electron and hole concentrations.

Matrix Form of Equations

Small-signal state equations (19) are a set of six simultaneous first-order linear differential equations in the complex space. These equations can be put into a matrix form as

$$\frac{d}{dx} \begin{bmatrix} V_p \\ V_n \\ V_i \\ J_p \\ J_n \\ J_i \end{bmatrix} = \begin{bmatrix} 0 & 0 & 0 & \frac{-1}{\sigma_p} & 0 & 0 \\ 0 & 0 & 0 & 0 & \frac{-1}{\sigma_n} & 0 \\ 0 & 0 & 0 & 0 & 0 & \frac{-1}{i\omega K_s E_0} \\ -i\omega c_p & 0 & i\omega c_p & 0 & 0 & 0 \\ 0 & -i\omega c_n & i\omega c_n & 0 & 0 & 0 \\ i\omega c_p & i\omega c_n & -i\omega c_p & 0 & 0 & 0 \end{bmatrix} \begin{bmatrix} V_p \\ V_n \\ V_i \\ J_p \\ J_n \\ J_i \end{bmatrix} \quad (21)$$

A complete small-signal equivalent circuit of the semiconductor region derived from these state equations has been presented. [7]

Boundary Values

The required boundary conditions for solving the above set of differential equations can be found by examining the boundaries at $x=0$ and $x=l$.

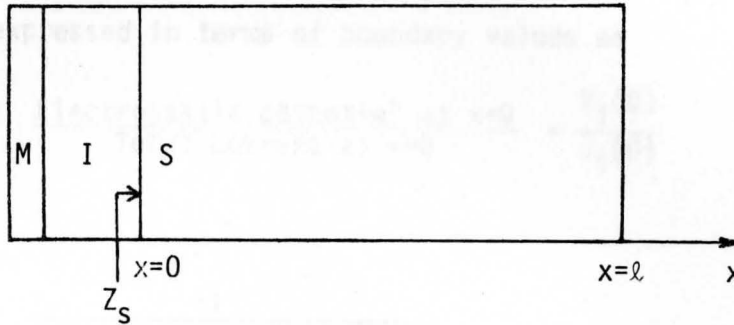


FIGURE 5. One Dimensional MIS Structure, showing Semiconductor Impedance and Boundaries.

At $x=0$, assumption of a perfect insulator and zero surface recombination dictates that $J_n(0) = J_p(0) = 0$. [4,8] These are the only boundary conditions that should be satisfied at the insulator-semiconductor interface. Looking at the other boundary, two situations are considered. First, assuming an ideal ohmic contact, which requires the electrostatic and Fermi potentials to be zero, [4]

$$V_i(l) = V_p(l) = V_n(l) = 0 \quad (22)$$

A non-ideal ohmic contact has also been modeled [7] and can be

formulated as

$$R_p = \frac{V_p(l)}{J_p(l)}$$

and

$$R_n = \frac{V_n(l)}{J_n(l)} \quad (23)$$

where R_p and R_n are ohmic contact resistances for holes and electrons, respectively.

The sixth boundary condition is arbitrary and for this problem it is taken as

$$J_i(\ell) = 1 \quad (\text{unit of current density})$$

Finally, the semiconductor impedance Z_s , capacitance C_s , and resistance R_s can be expressed in terms of boundary values as

$$Z_s = \frac{\text{Electrostatic potential at } x=0}{\text{Total current at } x=0} = \frac{V_i(0)}{J_i(0)} \quad (24)$$

and

$$\omega C_s = \frac{-1}{\text{Imaginary part of } (Z_s)} \quad (25)$$

$$R_s = \text{Real part of } (Z_s) \quad (26)$$

CHAPTER IV

NUMERICAL SOLUTION OF SMALL-SIGNAL STATE EQUATIONSGeneral Solution

A general homogenous linear boundary value problem may be expressed in the form [9]

$$\frac{dy}{dx} = \underline{A}(x)\underline{y} \quad (27)$$

where \underline{A} is an n by n matrix and \underline{y} is a vector of length n with the boundary conditions

$$\underline{B}\underline{y}(\ell) = \underline{D} \quad (28)$$

$$\underline{C}\underline{y}(0) = \underline{E} \quad (29)$$

\underline{B} is an $n-r$ by n matrix of rank $n-r$. \underline{C} is a r by n matrix of rank r .

\underline{D} and \underline{E} are vectors of length $n-r$ and r , respectively, containing the boundary values at $x=0$ and $x=\ell$. For the above linear homogenous problem the solution may be written in the form [8,9]

$$\underline{y}(x) = \underline{Z}(x) + \beta_1 \underline{y}^1(x) + \beta_2 \underline{y}^2(x) + \dots + \beta_r \underline{y}^r(x) \quad (30)$$

where \underline{y}^k are linearly independent solutions and β_k are the corresponding combining constants. Furthermore, expressing these solution as columns of matrix $\underline{Y}(x)$ and the constants as a vector $\underline{\beta}$, (30) may be written as

$$\underline{y}(x) = \underline{Z}(x) + \underline{Y}(x)\underline{\beta} \quad (31)$$

\underline{Y} having rank r and $\underline{\beta}$ being of length r . The solution $\underline{Z}(x)$ satisfies the homogenous equation and represents the particular solution that should satisfy the boundary condition at $x=\ell$. [8] At $x=\ell$, $\underline{Z}(\ell)$ is chosen so that it satisfies

$$\underline{B}\underline{Z}(\ell) = \underline{D} \quad (32)$$

forcing $\underline{Y}(\ell)$ necessarily to satisfy

$$\underline{B}\underline{Y}(\ell)\underline{\beta} = 0 \quad (33)$$

Applying the boundary relation (29), at $x=0$, one obtains

$$\underline{C}[\underline{Z}(0) + \underline{Y}(0) \cdot \underline{\beta}] = \underline{E} \quad (34)$$

The variables $\underline{Z}(\ell)$, $\underline{Y}(\ell)$ and $\underline{\beta}$ then are determined by (32-34).

Numerical Procedure

A scheme of solution can be classified as follows:^[8]

- 1) A vector $\underline{Z}(\ell)$ is chosen so that it satisfies (32); then the homogenous equation is integrated for \underline{Z} from $x=\ell$ to $x=0$, with $\underline{Z}(\ell)$ as the initial vector, to obtain $\underline{Z}(0)$;
- 2) r vectors of length n which are linearly independent are chosen (they shall be the r columns of $\underline{Y}(\ell)$) which satisfy $\underline{B} \underline{Y}(\ell) = 0$. This insures that (33) is satisfied for non-zero $\underline{\beta}$;
- 3) Each column of \underline{Y} is integrated backward from $x=\ell$ to $x=0$ to obtain $\underline{Y}(0)$;
- 4) Relation (34) is applied at $x=0$ with the solutions obtained in steps (1) - (3) and $\underline{\beta}$ is solved from (34) as

$$\underline{\beta} = [\underline{C} \underline{Y}(0)]^{-1} \cdot [\underline{E} - \underline{C} \underline{Z}(0)] \quad (35)$$

The constants β thus obtained will hold for $0 \leq x \leq \ell$ and the solution $\underline{y}(x)$ for any x in this region may be found by using $\underline{Y}(x)$, $\underline{Z}(x)$ and $\underline{\beta}$ in (31). This method essentially solves the boundary value problem as if it were an initial value problem.^[8,9]

Reconditioning

From the theory of linear ordinary differential equation, it is known that if one begins integration with a set of independent boundary value vectors, the solution vectors will then remain linearly independent through the course of integration.^[10] This insures that at $x=0$, $\underline{C} \underline{Y}$ will have an inverse and β may be found unambiguously.

Numerical implementation of this procedure to the problems being considered causes two kinds of difficulties. First, the assurance of continued linear independence of solution vectors can be made only if the integration is performed with infinite precision. Since machines have finite precision, even in a stable numerical method of integration the accumulation of round-off errors may cause the solution vectors to become linearly dependent.^[11] Even if linear independence is not lost, but the vectors in $\underline{Y}(0)$ come sufficiently close together such that $\underline{C} \underline{Y}(0)$ has a high condition number, great difficulty may be expected in accurately finding its inverse and $\underline{\beta}$.^[12] Secondly, even if $\underline{\beta}$ is accurate to the number of figures obtained, there is still another difficulty, because equation (30) will have combining numbers which are large compared to the desired solution. Hence, significance will be lost through subtraction.^[9] This error can not be avoided by a more accurate integration procedure unless at the same time extra precision is carried in all computations. Another method^[13] for avoiding loss of significance which does not require multiprecision arithmetic proposes that the matrix $\underline{Y}(x)$ of base solutions be kept orthogonal at each step of the integration. Another technique^[9] suggests that at each step of integration the base solutions and the particular solution be examined and when the base solutions exceed certain nonorthogonality criteria, the base and the particular solutions be orthonormalized. This method is used for the solution of small-signal state equations.

Applications to MIS Problem

Comparing (20-23) to the general boundary value problem given by (27-29), it can be seen that

$$n = 6 \quad r = 2 \quad \text{and} \quad \underline{y} = \begin{bmatrix} V_p \\ V_n \\ V_i \\ J_p \\ J_n \\ J_i \end{bmatrix} \quad (36)$$

The relation, $J_n(0) = J_p(0) = 0$, which describes the boundary relation at $x=0$ can be put in the form suggested by (29), where

$$\underline{C} = \begin{bmatrix} 0 & 0 & 0 & 1 & 0 & 0 \\ 0 & 0 & 0 & 0 & 1 & 0 \end{bmatrix} \quad \text{and} \quad \underline{E} = \begin{bmatrix} 0 \\ 0 \end{bmatrix} \quad (37)$$

Then assuming an ideal ohmic contact the boundary values at $x=l$ can be described in the general form (28) where

$$\underline{B} = \begin{bmatrix} 1 & 0 & 0 & 0 & 0 & 0 \\ 0 & 1 & 0 & 0 & 0 & 0 \\ 0 & 0 & 1 & 0 & 0 & 0 \\ 0 & 0 & 0 & 0 & 0 & 1 \end{bmatrix} \quad \text{and} \quad \underline{D} = \begin{bmatrix} 0 \\ 0 \\ 0 \\ 1 \end{bmatrix} \quad (38)$$

A non-ideal ohmic contact can also be described as above, where

$$\underline{B} = \begin{bmatrix} 1 & 0 & 0 & -R_p & 0 & 0 \\ 0 & 1 & 0 & 0 & -R_n & 0 \\ 0 & 0 & 1 & 0 & 0 & 0 \\ 0 & 0 & 0 & 0 & 0 & 1 \end{bmatrix} \quad \text{and} \quad \underline{D} = \begin{bmatrix} 0 \\ 0 \\ 0 \\ 1 \end{bmatrix} \quad (39)$$

Initial Vectors

According to previous discussions, three initial vectors should be designated, $\underline{Z}(l)$, $\underline{y}^1(l)$ and $\underline{y}^2(l)$, such that $\underline{BZ}(l) = \underline{D}$ and $\underline{B} \underline{Y}(l) = 0$.

First, assuming an ideal ohmic contact, these vectors can be found as

$$\underline{Z}(\ell) = \begin{bmatrix} 0 \\ 0 \\ 0 \\ 0 \\ 0 \\ 1 \end{bmatrix} \quad \underline{y}^1(\ell) = \begin{bmatrix} 0 \\ 0 \\ 0 \\ 1 \\ 0 \\ 0 \end{bmatrix} \quad \text{and} \quad \underline{y}^2(\ell) = \begin{bmatrix} 0 \\ 0 \\ 0 \\ 0 \\ 1 \\ 0 \end{bmatrix} \quad (40)$$

For a non-ideal ohmic contact these vector are:

$$\underline{Z}(\ell) = \begin{bmatrix} 0 \\ 0 \\ 0 \\ 0 \\ 0 \\ 1 \end{bmatrix} \quad \underline{y}^1(\ell) = \begin{bmatrix} R_p \\ 0 \\ 0 \\ 1 \\ 0 \\ 0 \end{bmatrix} \quad \text{and} \quad \underline{y}^2(\ell) = \begin{bmatrix} 0 \\ R_n \\ 0 \\ 0 \\ 1 \\ 0 \end{bmatrix} \quad (41)$$

Numerical Methods Used

As can be seen from (20) the elements of matrix A are all dependent on P and N. P and N are the static, spatial, concentration of electrons and holes, respectively. Unfortunately P and N can not be expressed in a closed form as a function of distance. But they can be expressed in terms of electrostatic potential which is given by (5). The relation between the electrostatic potential and distance is given in an integral form (14).

The region between $x=0$ and $x=\ell$ is divided in terms of the normalized potential, U, Figure 6. Then the corresponding subintervals are translated in terms of variable, x, by relation (8 and 14). It is clear that this method will not produce equal length subintervals, which in this case

is an advantage, because it gives intervals that become smaller as one moves toward the surface of the semiconductor. The region between $x=0$ and $x=l$ is divided into two sections called surface region and the bulk. The transition between the surface and the bulk is chosen to be where the electrostatic potential reaches $1/300$ of its surface value.

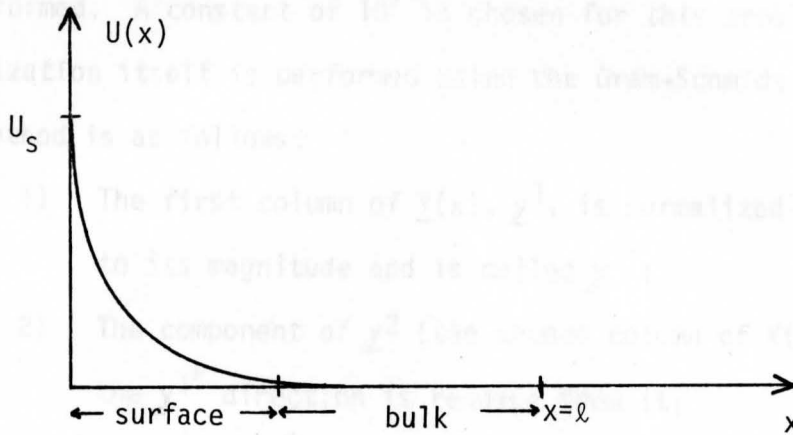


FIGURE 6. U Versus x showing Surface and Bulk Regions

The surface region is divided into equal increments of normalized electrostatic potential, U . The bulk is divided into equal increments of distance, x . The ratio of the number of subintervals in the surface region to the number of subintervals in the bulk is chosen to be $5/2$.

Method of Integration

Whereas any reasonable scheme of integration which exhibits stability over the region of computation may be used, a simple predictor-corrector method^[11] is used here. Considering integration over any two grid points I and $I+1$ with solutions $\underline{y}(I)$, $\underline{y}(I+1)$ and grid length $Dx(I)$, and remembering that the integration is performed backward, the prediction step will be

$$\underline{y}_p = \underline{y}(I) - Dx(I)[\underline{A}(I)\underline{y}(I)] \quad (42)$$

where \underline{y}_p is the intermediate solution vector. The correction step is

$$\underline{y}^{(I+1)} = \underline{y}^{(I)} - \Delta x^{(I)} [\underline{A}^{(I)} \underline{y}^{(I)} + \underline{A}^{(I+1)} \underline{y}_p] / 2 \quad (43)$$

Method of Orthonormalization

To check for the need of orthonormalization the criteria explained by [9] is used. This method states simply that when the magnitude of any vector in $\underline{Y}(x)$ exceeds a preassigned constant an orthonormalization must be performed. A constant of 10^7 is chosen for this problem. The orthonormalization itself is performed using the Gram-Schmidt method. [14]

This method is as follows:

- 1) The first column of $\underline{Y}(x)$, \underline{y}^1 , is normalized with respect to its magnitude and is called \underline{y}^{1*} ;
- 2) The component of \underline{y}^2 (the second column of $\underline{Y}(x)$) which lies in the \underline{y}^{1*} direction is removed from it;
- 3) To obtain \underline{y}^{2*} , the vector obtained above is normalized with respect to its magnitude;
- 4) The same process is repeated for \underline{y}^3 . The components of \underline{y}^3 in the \underline{y}^{1*} and \underline{y}^{2*} directions are removed from it and then \underline{y}^3 is normalized.

The vectors \underline{y}^{1*} , \underline{y}^{2*} and \underline{y}^{3*} are orthogonal and of unit magnitude.

In the case of small-signal state equations, these vectors have complex components. The scalar product for these vectors is carried out the same way as vectors in the real space.

CHAPTER V

RESULTS

A computer program based on the discussion of the previous chapter for solving the small-signal state equations was prepared. This program is composed mainly of two parts (see Appendix A). In the first part, the static solution given by (11) is found. In the second part the state equations are treated like a boundary value problem and solved. The semiconductor impedance, Z_s , is found and the whole MIS structure is modeled by the circuit shown in Figure 7(c).

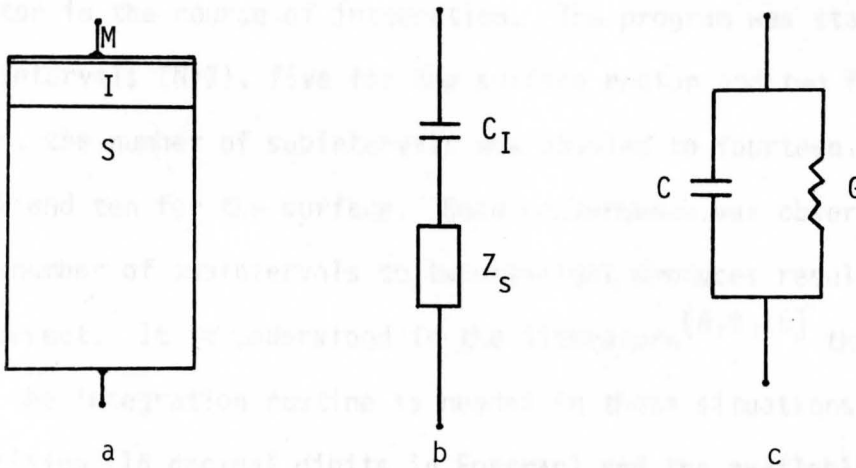


FIGURE 7. Equivalent Circuit of the MIS Structure

$$C = \frac{C_t}{1 + \omega^2 C_t^2 R_s^2} \quad G = \frac{\omega^2 C_t^2 R_s}{1 + \omega^2 C_t^2 R_s^2} \quad (44)$$

where

$$C_t = \frac{C_s C_I}{C_s + C_I} \quad C_s = \frac{-1}{\omega \text{Imag}(Z_s)}$$

and $R_s = \text{Real}(Z_s)$

Numerical values for C/C_I for different insulator thicknesses, frequencies and doping levels is found and C-V curves are obtained. An ideal ohmic contact is assumed for these cases. A non-ideal ohmic contact is also modeled and C-V characteristics for different ohmic contacts are obtained. The insulator thickness, x_I , and doping level, U_F , used in these examples are chosen from typical values for MIS structures. [1,4]

Convergence of the Method

Even though the orthonormalization process is used to prevent the need of multiprecision arithmetic, the precision comes to be an important factor in the course of integration. The program was started with seven subintervals ($N=7$), five for the surface region and two for the bulk. Then, the number of subintervals was doubled to fourteen, four for the bulk and ten for the surface. Good convergence was observed. Doubling the number of subintervals to twenty-eight produces results which are incorrect. It is understood in the literature [8,9,15] that more precision for the integration routine is needed in these situations. Using double precision (16 decimal digits in Fortran) and the available IBM 370 system, it was not possible to go further than fourteen subintervals. Of course some changes to the location and number of reconditioning points may improve the results. The results for ($N=14$) are given in Figure 8. In this figure the charge-analysis approach is compared to the results of the numerical solution of small-signal state equations for $\text{SiO}_2\text{-Si}$. In this example using $8.15 \Omega\text{-cm Si}$, the minority carrier response for 100kHz is low enough that the difference between charge analysis and the solution of state equations can be considered to be due to the convergence of the method that is used and the computer limitations. As can be seen the results of state equations compare very well in accumulation and

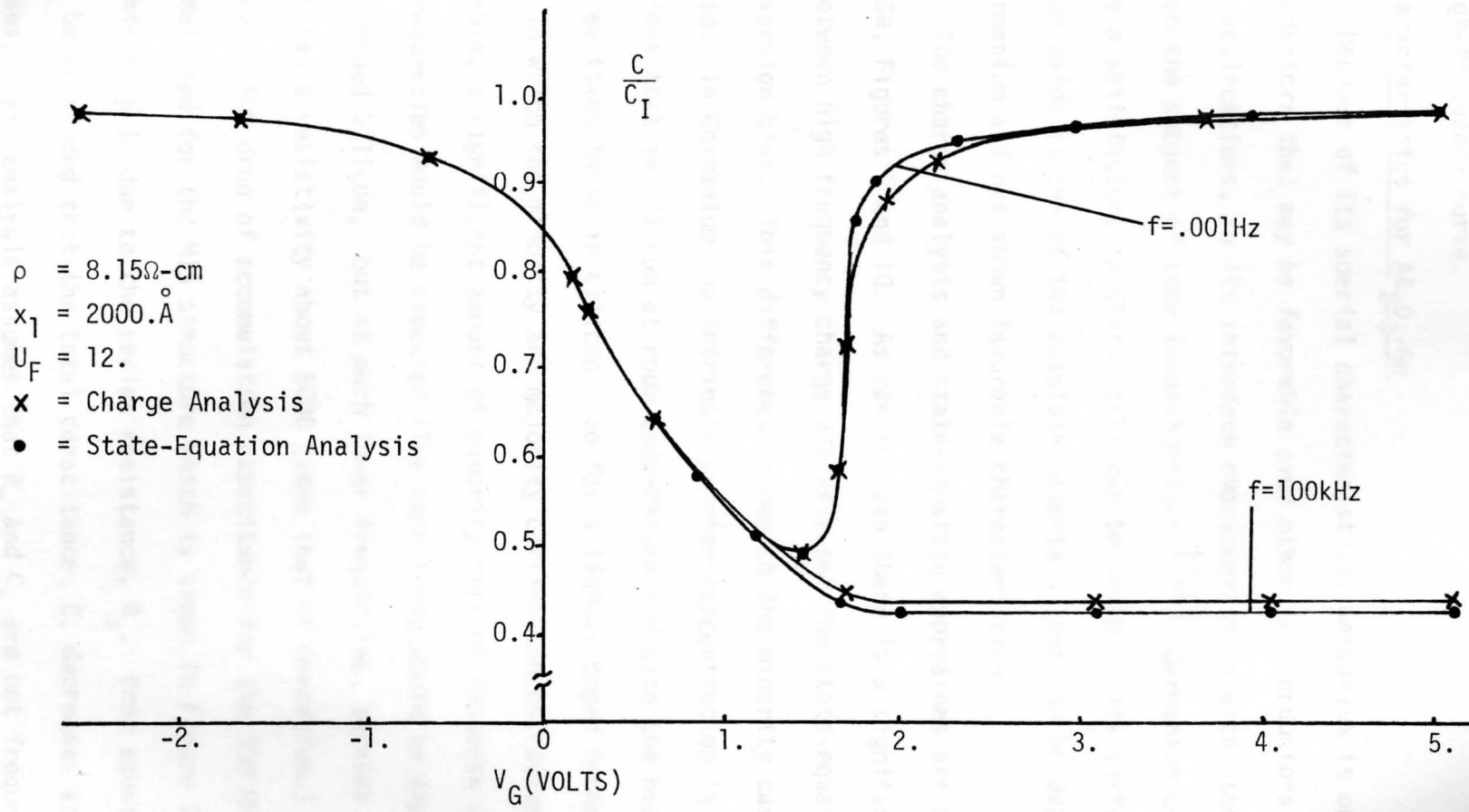


FIGURE 8. Charge Analysis versus State-Equation Approach for $\text{SiO}_2\text{-Si}$, $N=14$.

depletion, but there is about 2.5% difference in the inversion region for the high-frequency curve.

C-V Characteristics for Al_2O_3 -Ge

Because of its special characteristics, Germanium is one of the semiconductors that may be favorable over other semiconductors for some device applications, so its interface characteristics with other insulators has been the subject of some investigations.^[1,2] Germanium can not provide a satisfactory insulator that can be grown on its surface. Aluminum oxide is one of the possible materials that can be deposited on the Germanium and has shown favorable characteristics.

The charge analysis and state-equation approaches are given for Al_2O_3 -Ge, Figures 9 and 10. As can be seen there is a significant difference between high-frequency charge analysis and the state-equation analysis for inversion bias. This difference is due to the minority carrier response. In Germanium the intrinsic carrier concentration is about 1800 times that in Silicon at room temperature and also the mobilities are three times those in silicon. So for a lightly doped Germanium substrate, in which the minority and majority carrier concentrations are comparable, a significant amount of minority carrier response even at high frequencies would be expected. (The same thing would be expected for lightly doped Silicon, but at much lower frequencies, because intrinsic silicon has a resistivity about 5000 times that of Germanium.) Figure 10 shows about 50% drop of accumulation capacitance for the 500 MHz curve. The model used for the MIS structure which is shown in Figure 7 suggests that this drop is due to the series resistance, R_s . From equation (44) it can be concluded that the total capacitance, C , decreases as frequency increases. This analysis assumes that R_s and C_t are not frequency dependent.

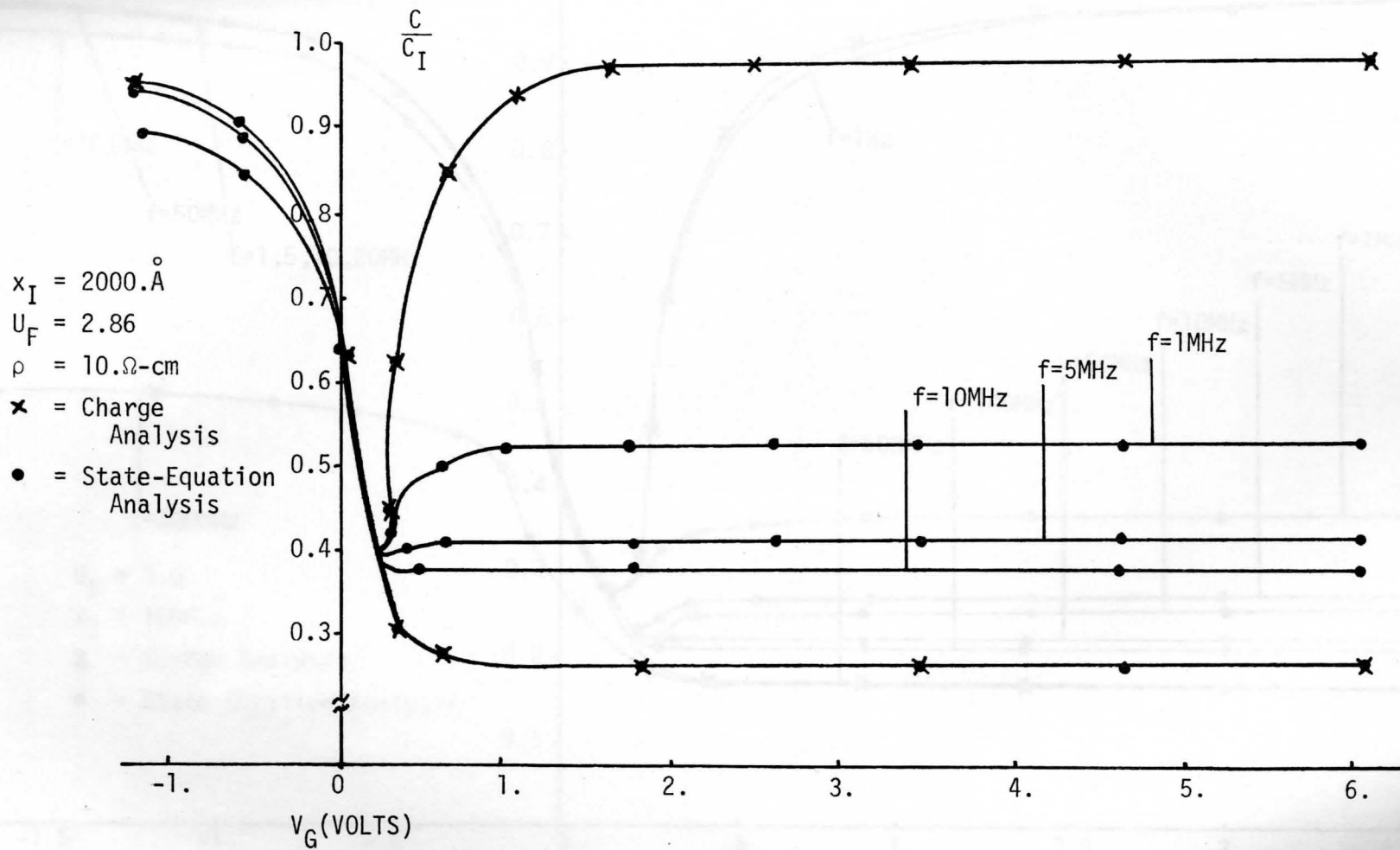


FIGURE 9. C-V Characteristics using Charge Analysis and State-Equation Approach for Al_2O_3 -Ge, p-type.

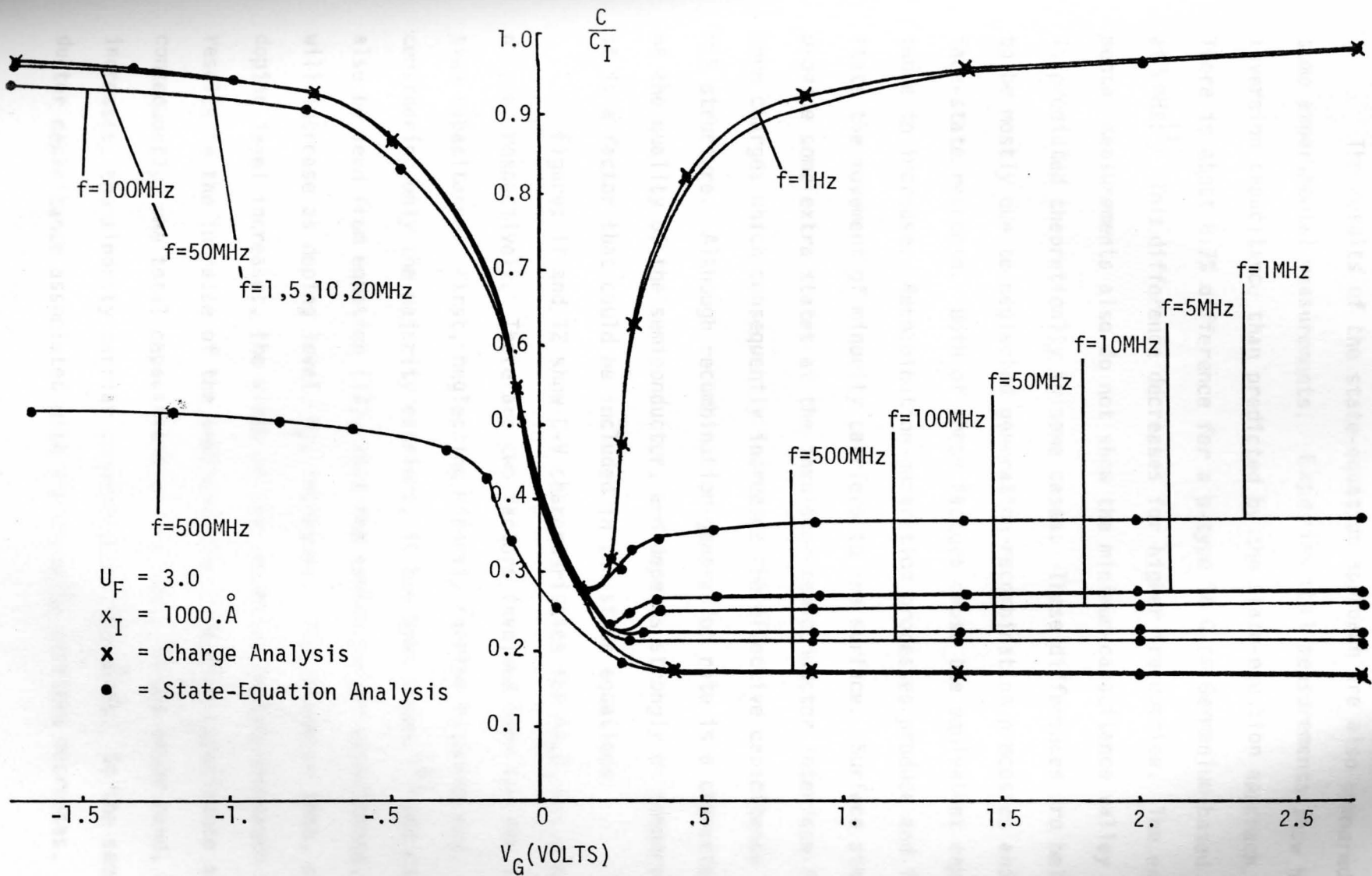


FIGURE 10. C-V Characteristics, showing Minority Carrier Response for $\text{Al}_2\text{O}_3\text{-Ge}$, p-type.

The results of the state-equation approach are also compared to some experimental measurements. Experimental measurements show higher inversion capacitance than predicted by the state-equation approach. There is about 8.7% difference for a p-type 16 Ω -cm Germanium-based device at 5 MHz.^[1] This difference decreases for higher frequencies. The experimental measurements also do not show the minimum-capacitance valley which is predicted theoretically in some cases. These differences are believed to be mostly due to neglected generation-recombination processes and surface-state response. Both of these factors cause the equivalent capacitance to increase. Recombination-generation processes produce and facilitate the movement of minority carriers to the surface. Surface states also provide some extra states at the insulator-semiconductor interface for more charges which consequently increases the effective capacitance of the MIS structure. Although recombination-generation rate is a characteristic of the quality of the semiconductor, and depends strongly on temperature,^[16] it is a factor that could be included in the state equations.

Figures 11 and 12 show C-V characteristics for Al_2O_3 -Ge, p and n type, respectively. There are two factors involved here for the inversion capacitance. First, neglecting minority carrier response and considering only the majority carriers, it has been shown,^[4] and can also be seen from equation (17), that the semiconductor capacitance, C_s , will increase as doping level, U_F , increases. The reason is that, as doping level increases, the width of the depletion region decreases which results in the increase of the semiconductor inversion capacitance and, consequently, the total capacitance of the MIS. On the other hand, as U_F increases, the minority carrier concentration decreases. So the semiconductor capacitance associated with the minority carriers decreases.

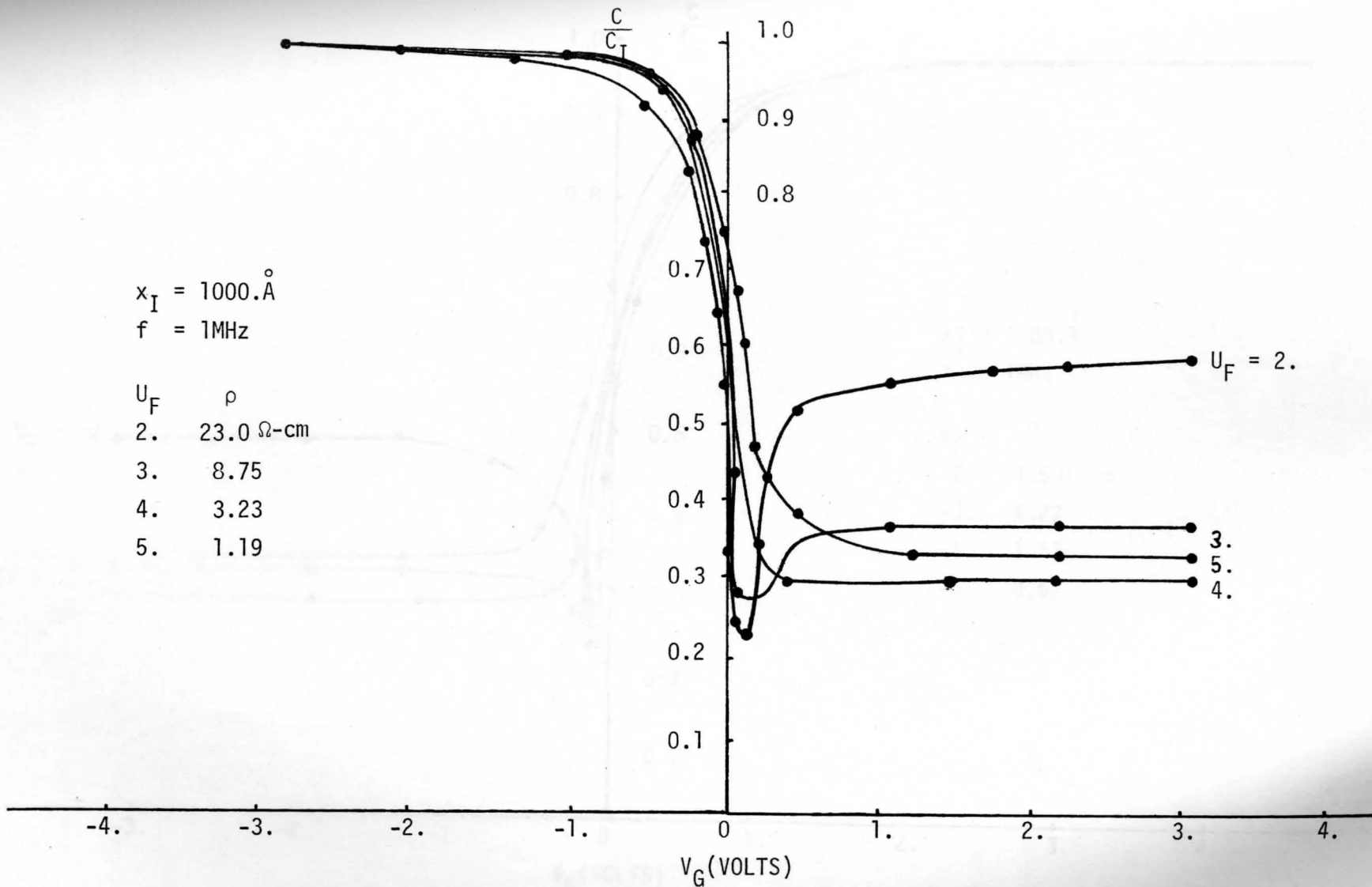


FIGURE 11. C-V Characteristics, showing Effect of Doping Level for $\text{Al}_2\text{O}_3\text{-Ge}$, p-type

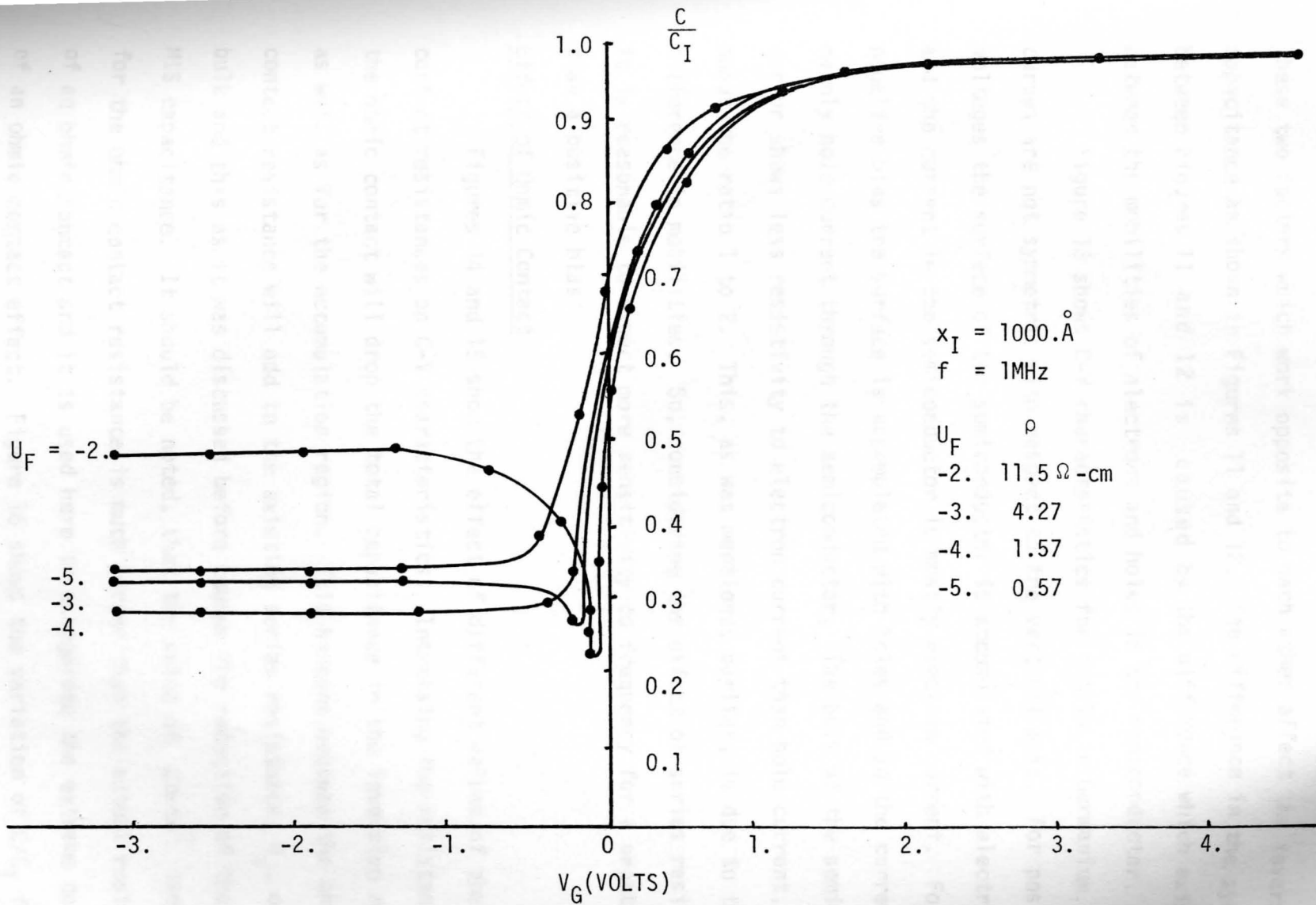


FIGURE 12. C-V Characteristics, showing Effect of Doping Level for $\text{Al}_2\text{O}_3\text{-Ge}$, n-type.

This results in the reduction of the equivalent capacitance of the MIS. These two factors which work opposite to each other affect the inversion capacitance as shown in Figures 11 and 12. The difference in the symmetry between Figures 11 and 12 is caused by the difference which exists between the mobilities of electrons and holes in the semiconductor.

Figure 13 shows C-V characteristics for intrinsic Germanium. The curves are not symmetric with respect to the vertical axis. For positive voltages the surface of the semiconductor is accumulated with electrons and the current in the semiconductor is mostly electron current. For a negative bias the surface is accumulated with holes and so the current is mainly hole current through the semiconductor. The bulk of the semiconductor shows less resistivity to electron current than hole current, about the ratio 1 to 2. This, as was mentioned earlier, is due to the difference in mobilities. So, considering the effect of series resistance it is reasonable to expect more sensitivity to frequency for a negative than a positive bias.

Effect of Ohmic Contact

Figures 14 and 15 show the effect of different values of ohmic contact resistances on C-V characteristics. Increasing the resistance of the ohmic contact will drop the total capacitance in the inversion region as well as for the accumulation region. This happens because the ohmic contact resistance will add to the existing series resistance, R_s , of the bulk and this as it was discussed before causes the reduction of the MIS capacitance. It should be noted, that the value of $2\Omega\text{-cm}^2$ used here for the ohmic contact resistance is much larger than the actual resistance of an ohmic contact and it is used here to exaggerate the extreme case of an ohmic contact effect. Figure 16 shows the variation of C/C_I for a fixed ohmic contact versus frequency for a point in inversion region.

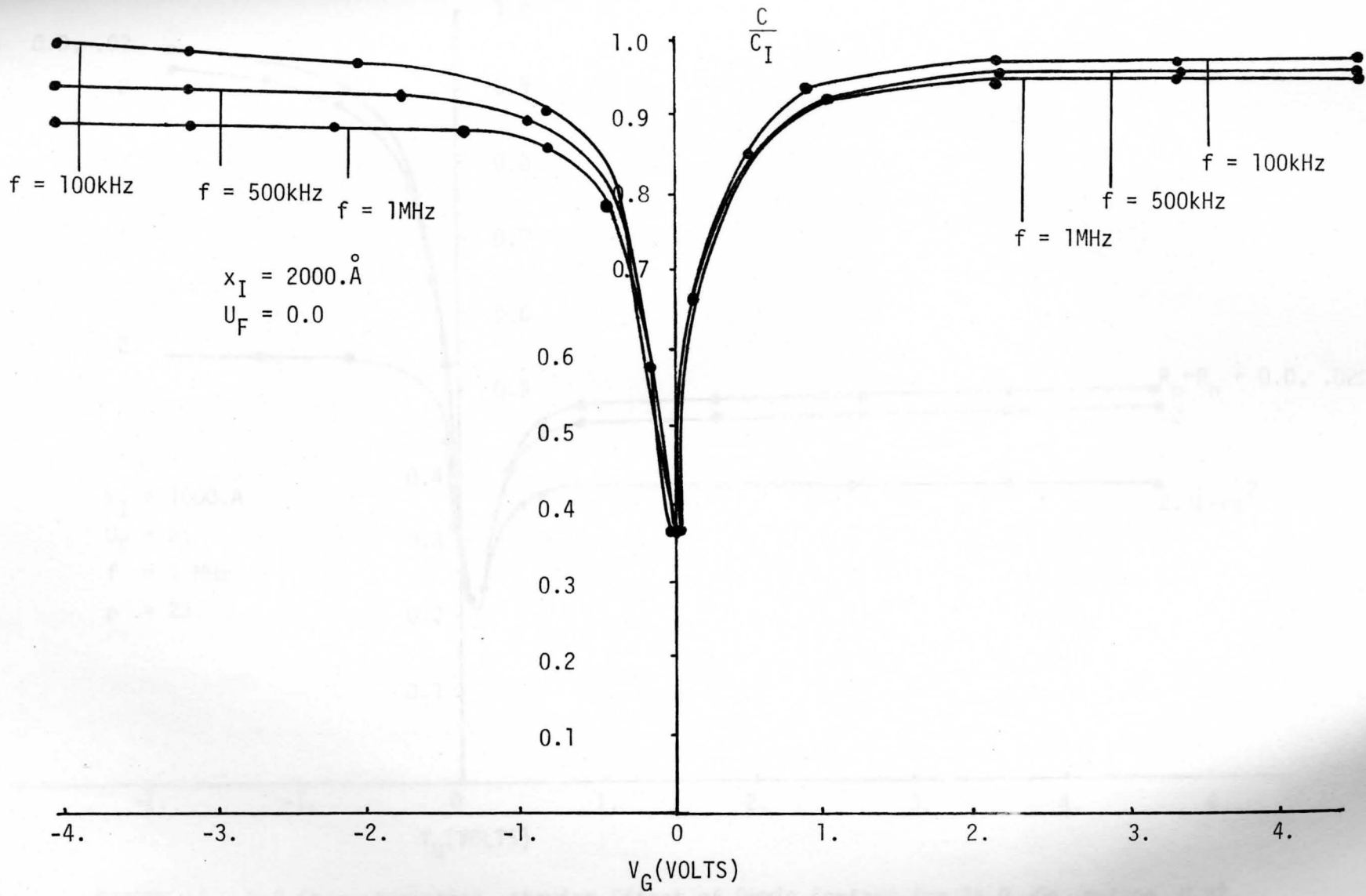


FIGURE 13. C-V Characteristics for $\text{Al}_2\text{O}_3\text{-Ge}$ (Intrinsic)

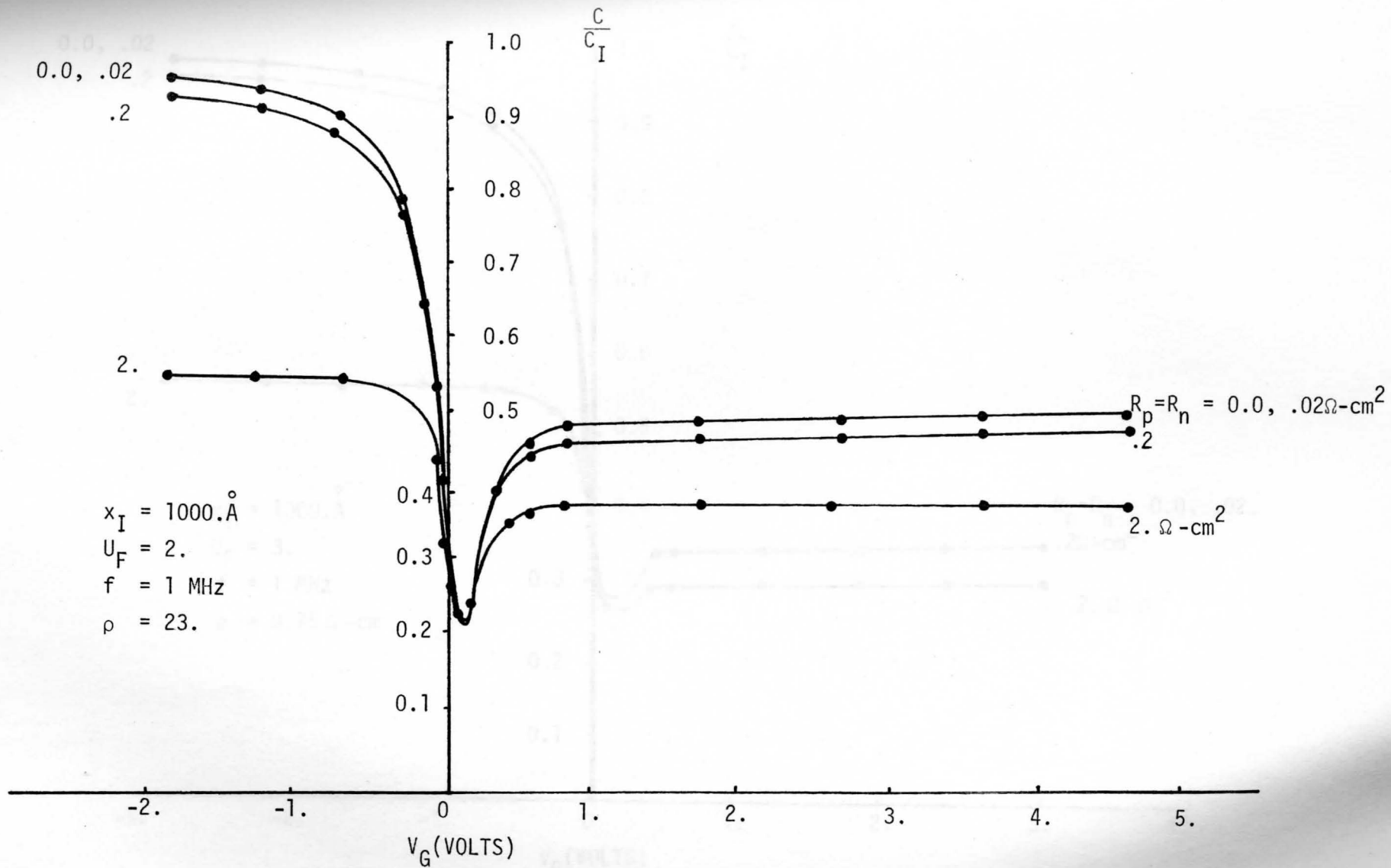


FIGURE 14. C-V Characteristics, showing Effect of Ohmic Contact for $\text{Al}_2\text{O}_3\text{-Ge}$, p-type, $U_F=2.$

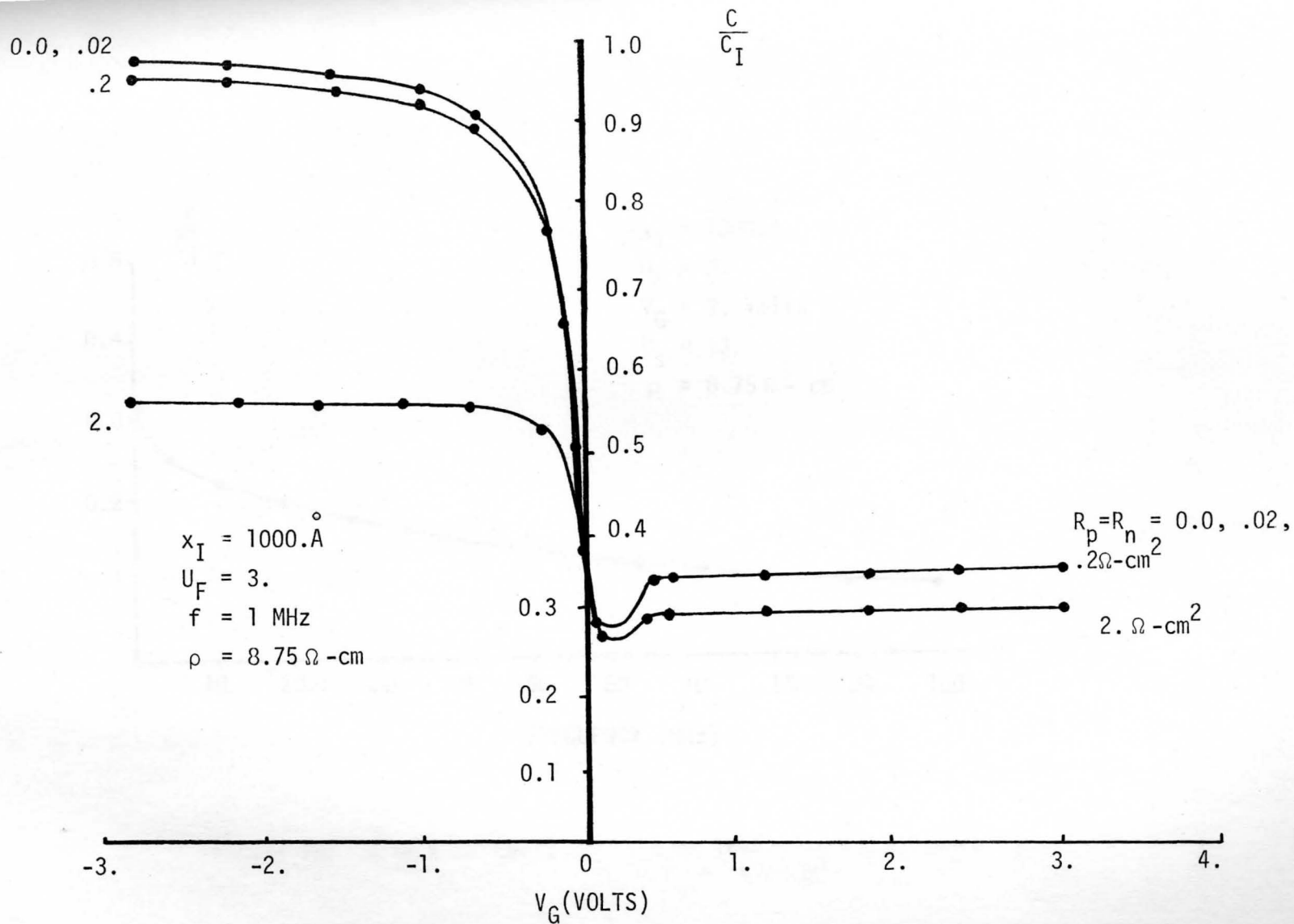


FIGURE 15. C-V Characteristics, showing Effect of Ohmic Contact for $\text{Al}_2\text{O}_3\text{-Ge}$, p-type, $U_F=3$.

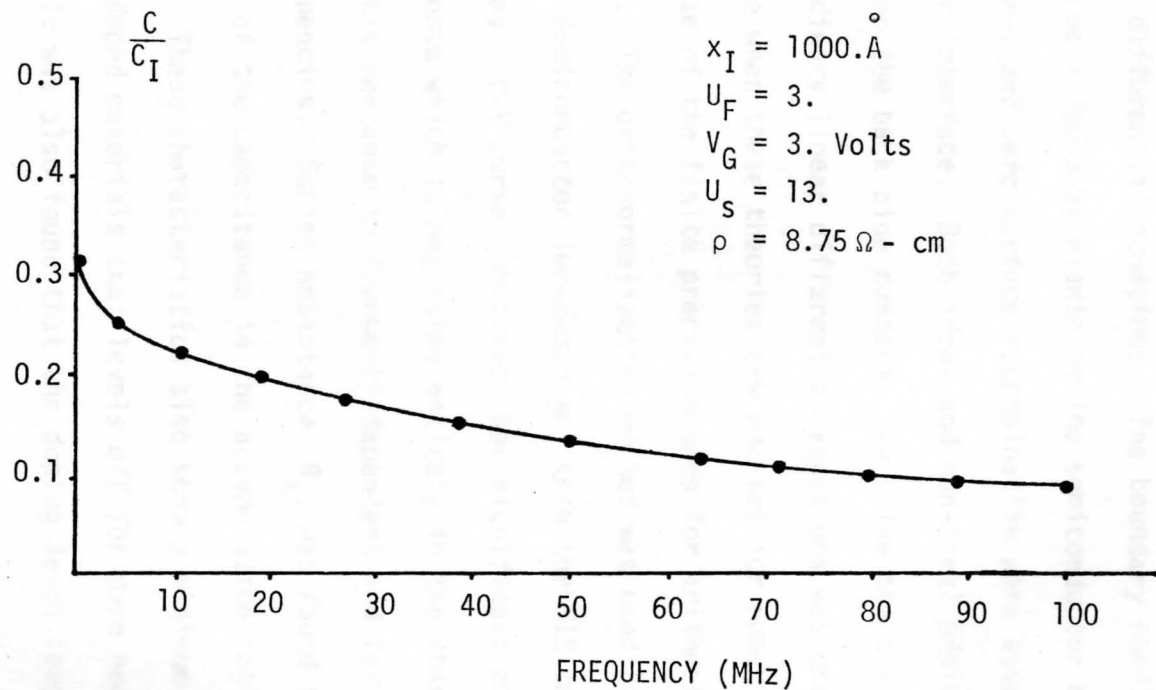


FIGURE 16. Effect of Ohmic Contact on Inverting Capacitance for $R_p = R_n = .02 \Omega - \text{cm}^2$

CHAPTER VI

SUMMARY, CONCLUSION AND SUGGESTIONS FOR FURTHER WORK

In this work a more complete way for analyzing MIS structures and a study of minority carrier response in these structures were presented. The behavior of charge carriers in the semiconductor for small excitation, which is given by small-signal state equations, was put into a set of first-order linear differential equations. The boundary conditions required for this problem were found by examining the semiconductor boundaries. Zero leakage current and zero surface recombination were assumed at insulator-semiconductor interface. Both ideal and non-ideal ohmic contacts were considered for the back side contact. To solve the state equations the theory of ordinary linear differential equations was used. Some difficulties arise when these theories are adapted for numerical calculations, mainly because of the finite precision used for arithmetic operations in computers. The orthonormalization method was used to reduce this deficiency. Semiconductor impedance and then the MIS capacitance were found this way. C-V curves obtained show significant amount of minority carrier response which is neglected entirely in the charge analysis approach. This response is frequency dependent and for Germanium extends to high frequencies. Series resistance, R_s , was found to be the reason for the drop of the capacitance in the accumulation region at very high frequencies. These characteristics also show a minimum-capacitance valley for lightly doped materials that levels off for more heavily doped materials. It was also found that the doping level coupled with the minority carrier response are the important factors in the determination of the inversion capacitance. Similar curves for n and p type materials

were obtained. These curves were not symmetric and this is due to the difference in carrier mobilities. C-V curves for intrinsic Germanium for different frequencies were also obtained. Finally, the effect of back ohmic contact was studied. A non-ideal ohmic contact reduces the capacitance both in accumulation and inversion biases. Increasing the ohmic contact resistance will increase this effect. It was also found that increasing the frequency will reduce the MIS capacitance for a fixed back ohmic contact.

Suggestions for Further Work

- 1) In small-signal state equations presented in Chapter III, the generation-recombination process was neglected, but it has been shown in [2] that it can be included in those equations and after some manipulation it can be put into a matrix form similar to (20).
- 2) Other methods for checking the need for orthonormalization, like monitoring the angle between vectors, which is discussed in [9] or even a periodical type of orthonormalization, could be studied.
- 3) The trap capacitance, c_t ,^[7] at the ohmic contact could be included by changing the boundary conditions at the ohmic contact properly.
- 4) In this work the thickness of the semiconductor substrate was fixed. Further work could also include a study of the effect of this factor.
- 5) A study to maximize the convergence of the method by changing the number of subintervals in the surface and bulk region could be done.

- 6) Finally, in order to get better results, the computer program given for the numerical solution of state equations could be run by machines that provide more than 16 decimal digits for arithmetic operations to check the convergence of the method.

LIST OF REFERENCES

1. S. I. Braginskii, "Interference of Al₂O₃-Ga Structures and Characteristics of High- μ M... Journal of Applied Physics, Vol. 50, No. 10, October 1971.
2. J. B. F. da Silva, "Statistics of Alchem... Microchemical Journal, Vol. 10, No. 1, 1969.
3. R. F. Pierret, Lectures on..., 1973.
4. K. H. Hellwarth, Journal of Applied Physics, Vol. 40, No. 26, pp. 3755-3757, 1969.
5. G. T. Sen, Journal of Applied Physics, Vol. 40, No. 10, pp. 3485-3486, 1969.
6. G. T. Sen, P. M. Chatterjee and A. K. Chatterjee, "Exact Analytical Solution of High- μ M... and Characteristics and Values of Charge... Journal of Applied Physics, Vol. 52, No. 9, pp. 541-543, September 1982.
7. A. C. Sparrow and J. N. Madala, "An Improved Numerical Method for the Solution of A.C. Analysis... IEEE Transactions on Electron Devices, Vol. 34, No. 1, December 1987.
8. G. D. Gasp, "The Numerical Solution of Ordinary Value Problems," SIAM Review, Vol. 8, No. 23, July 1966.
9. L. Fox, Numerical Solution of Partial Differential Equations in Science and Engineering, Oxford University Press, 1962.
10. W. S. Duggins, Numerical Methods for Scientists and Engineers, New York: McGraw-Hill, 1973.
11. G. E. Forsythe and W. M. Marsden, Computer Methods for Partial Differential Equations, Prentice-Hall, 1970.
12. A. G. Kurov, "On the Theory of General Solution of Boundary Value Problems for Systems of Linear Ordinary Differential Equations," Ukrainian Math. Journal, No. 19, 1971.
13. R. Courant, E. O. Ritz, and F. W. Clow, Field Variables for Engineers, New York: Wiley, 1965.
14. R. S. Steihaug and A. Watts, "Computational Solution of Linear and Nonlinear Boundary Value Problems via Orthogonalization," IEEE Transactions on Numerical Analysis, Vol. 14, No. 1, March 1987.

LIST OF REFERENCES

1. P.C. Munro, Ph.D. dissertation, Purdue University, 1973.
2. S. Iwauchi and T. Tanaka, "Interface Properties of Al_2O_3 -Ge Structure and Characteristics of Al_2O_3 -Ge MOS Transistors," Japanese J. Applied Physics, Vol. 10, #2, pp. 260-265, Feb. 1971.
3. S. Krongelb, "Stability of Aluminum Oxide Films on Ge Devices," J. Electrochemical Soc., Vol. 116, #11, pp. 1583-1584, Nov. 1969.
4. R.F. Pierret, Lecture Notes, used at Purdue University, 1973.
5. E.H. Nicollian and A. Goetzberger, Bell System Technical J., Vol. 46, #6, pp. 1055-1133, 1967.
6. C.T. Sah, Proc. IEEE #55, pp. 654, 1967.
7. C.T. Sah, R.F. Pierret and A.B. Tole, "Exact Analytical Solution of High Frequency Lossless MOS Capacitance-Voltage Characteristics and Validity of Charge Analysis," Solid State Electronics, Vol. 12, #9, pp. 681-688, September 1969.
8. A.G. Fortino and J.N. Nadan, "An Efficient Numerical Method for the Small-Signal A.C. Analysis of MOS Capacitors," IEEE Transaction on Electron Devices, Vol. ED-24, #9, September 1977.
9. S.D. Conte, "The Numerical Solution of Linear Boundary Value Problems," SIAM Review, Vol. 8, #3, July 1966.
10. L. Fox, Numerical Solution of Two Point Boundary Problems in Ordinary Differential Equations, London, England: Oxford University Press, 1957.
11. R.W. Hamming, Numerical Methods for Scientists and Engineers, New York: McGraw-Hill, 1973.
12. G.E. Forsythe and W. Wasour, Finite-Difference Methods for Partial Differential Equations. New York: Wiley, 1960.
13. S. Godunov, "On the Theory of Numerical Solution of Boundary Value Problems for Systems of Linear Ordinary Differential Equations," Uspehi Mat. Nauk, 16. 1961.
14. P.M. Derusso, D.J. Roy, and C.M. Close, State Variables for Engineers, New York: Wiley, 1965.
15. M.R. Scott and H.A. Watts, "Computational Solution of Linear Two Point Boundary Value Problems Via Orthonormalization," SIAM J. Numerical Analysis, Vol. 14, #1, March 1977.

REFERENCES (Continued)

16. U.K. Kelberlau and R. Kassing, "Theory of Nonequilibrium Properties of MIS Capacitors Including Charge Exchange of Interface States with Both Bands," Solid State Electronics, Vol. 22, 1978.
17. S.M. Sze, Physics of Semiconductor Devices, Wiley Interscience, 1969.
18. C. Kittel, Introduction to Solid State Physics, 5th Edition, Wiley, 1976.
19. F. Scheid, Theory and Problems of Numerical Analysis, McGraw-Hill, 1968.
20. I.S. Sokolnikoff and R.M. Redheffer, Mathematics of Physics and Modern Engineering, 2nd Edition, McGraw-Hill, 1966.
21. S.M. Roberts and J. Shipman, Two Point Boundary Value Problems, (Shooting Methods, Modern Analytical and Computational Methods in Science and Mathematics, No. 31). New York, American Elsevier, 1972.
22. P.W. Murrill and C.L. Smith, Introduction to Computer Science, Intext Educational Publishers, 1973.

APPENDIX A
STATE-ELECTION PROGRAM

APPENDICES

This process is composed of three parts. The first part gives the required constants and generalizes the relationships which are needed for this process. Part two, solves the static equations given by relation (14) and does the job of partitioning the variables. The integration required in (14) is performed by a technique described in the appendix. Part three solves the small-signal equations and is described in the appendix. The procedure outlined in Chapter 10 is used to solve the equations provided by the submatrix RL . The information needed by this procedure is provided using a predictor-corrector method by equation (10). Submatrix $RLTN$ takes care of the ortho-normalization whenever it is needed.

APPENDIX A

STATE-EQUATION PROGRAM

This program is composed of three parts. The first part gives the required constants and generates the parameters which are needed for this problem. Part two, solves the static equation given by relation (14) and does the job of partitioning the range of x . The integration required in (14) is performed by subprogram AI using Simpson's rule. Part three solves the small-signal state equations given by (27). The procedure outlined in Chapter IV is used. Matrix A is produced by the subroutine FILL. The integrations needed in this procedure are performed using a predictor-corrector method by subroutine PC. Subroutine ORTHN takes care of the orthonormalization whenever it is needed.

```

K=16.
K=0.

```

```

DOPIAP LEVEL AND OPERATIONS

```

```

US=1.
PRO=10.0

```

```

SUBROUTINE REQUIRED PARAMETERS

```

```

JCONP=1.0/2.0
W=0.01/2.0
JCONK
OPE=1.0/2.0
JNO=1.0/2.0
JACK=1.0/2.0
JCK=1.0/2.0

```

```

T=0.0
EUP=1.0/2.0
RIG=1.0/2.0
L=0.0
K=0.0
R=0.0

```

```

N=16
M=8
K=1

```

```

K=1.0/2.0

```

```

1.0/2.0

```

```

REAL NI,K,KO,KS,MP,MN,LD,KTQ,KSXOLD
REAL*8 DX(14),X,XS,U(15),US,SUS
COMPLEX A1(6,6),A2(6,6),J,JW,JWC,JWCK,CMLX
COMPLEX*16 Z(6),Y1(6),Y2(6),VI,JI,ZS,DET,B1,B2
COMMON EUF /LIST1/ LD /LIST2/ QP,QN,JWCK,JWC

```

```

C
C PHYSICAL CONSTANTS AND TEMPERATURE
C

```

```

Q=1.60219E-19
K=1.38062E-23
E0=8.8542E-14
T=296.

```

```

C
C DIMENSIONS OF THE DEVICE
C

```

```

X=12.70E-3
X0=1.E-5

```

```

C
C SEMICONDUCTOR AND INSULATOR CONSTANTS
C

```

```

NI=1.8595E13
MP=1900.
MN=3900.
KS=16.
KO=8.

```

```

C
C DOPING LEVEL AND OPERATING POINT
C

```

```

UF=3.
US=-9.
FRQ=100.E4

```

```

C
C GENERATING REQUIRED PARAMETERS
C

```

```

J=CMLX(0.0,1.)
W=2.*3.14*FRQ
JW=J*W
QP=-1./(Q*MP*NI)
QN=-1./(Q*MN*NI)
JWCK=-1./(JW*KS*E0)
JWC=(JW*(Q**2)*NI)/(K*T)
CO=KO*E0/X0
EUF=EXP(UF)
KTQ=K*T/Q
LD=SQRT((KS*E0*K*T)/(2.*(Q**2)*NI))
KSXOLD=(KS*X0)/(KO*LD)
RES=1./(Q*NI*(MP*EUF+MN/EUF))

```

```

N=14
M=2*N/7
M1=M+1
M2=M+2

```

```

WRITE(6,11) FRQ,UF,RES
11 FORMAT(1H1///,13X,'FREQUENCY(HZ)=' ,3PE8.0,' , UF=' ,
1' , RESISTIVITY(OHM-CM)=' ,0PF10.6///20X,' C/CO

```

°PF5.2

```

      2          VG')
C
C   STARTING PROGRAM CALCULATIONS
C
13 CONTINUE
   SUS=US/DABS(US)
   VG=SNGL(KTQ*(US+SUS*KSXOLD*F(US)))
C
C   GENERATING U(I)
C
      DO 2 I=1,M
      U(I)=0.0
2 CONTINUE
   U(M+1)=US/300.
   U(M+2)=US/(N-M)
      DO 3 I=M2,N
      U(I+1)=U(I)+U(M+2)
3 CONTINUE
C
C   GENERATING DX(I)
C
      XS=0.0
      DO 4 I=M1,N
      DX(I)=AI(U(I+1),U(I))
      XS=XS+DX(I)
4 CONTINUE
   DX(M)=(X-XS)/M
      DO 5 I=1,M
      DX(I)=DX(M)
5 CONTINUE
   GO TO 44
33 DO 22 I=1,15
22 U(I)=0.0
C
C   ASSIGNING INITIAL VALUES TO VECTORS Z,Y1,Y2
C
44 DO 1 I=1,6
   Z(1)=CMPLX(0.0,0.0)
   Y1(I)=CMPLX(0.0,0.0)
   Y2(I)=CMPLX(0.0,0.0)
1 CONTINUE
   Z(6)=CMPLX(1.,0.0)
   Y1(4)=CMPLX(1.,0.0)
   Y2(5)=CMPLX(1.,0.0)
C
C   INTEGRATING Z,Y1,Y2 FROM POINT 1 TO N
C
      CALL FILL(A1,U(1),1)
      DO 6 L=1,N
      CALL FILL(A2,U(I+1),2)
      CALL PC(Z,A1,A2,DX(I))
      CALL PC(Y1,A1,A2,DX(I))
      CALL PC(Y2,A1,A2,DX(I))
      DO 7 L=1,6

```

 DO 7 MM=1,6

 A1(L,MM)=A2(L,MM)

 7 CONTINUE

 C
 C CHECKING FOR ORTHONORMALIZATION

 T1=10.E7

 T2=REAL(Z(3))**2+AIMAG(Z(3))**2

 T3=REAL(Y1(3))**2+AIMAG(Y1(3))**2

 T4=REAL(Y2(3))**2+AIMAG(Y2(3))**2

 IF(T2.GE.T1.OR.T3.GE.T1.OR.T4.GE.T1) CALL ORTHN(Z,Y1,Y2)

 6 CONTINUE

 C
 C FINDING B1,B2

 DET=Y1(4)*Y2(5)-Y1(5)*Y2(4)

 B1=(Y2(4)*Z(5)-Y2(5)*Z(4))/DET

 B2=(Y1(5)*Z(4)-Y1(4)*Z(5))/DET

 C
 C FINDING VI,JI,ZS,CPC0

 VI=Z(3)+B1*Y1(3)+B2*Y2(3)

 JI=Z(6)+B1*Y1(6)+B2*Y2(6)

 ZS=VI/JI

 CPC0=REAL(1./(1.+JW*C0*ZS))

 WRITE(6,17) CPC0,US,VG

 17 FORMAT(1H0,20X,F9.7,8X,F4.0,8X,F10.6)

 US=US+1.

 IF(US.EQ.0.0) GO TO 33

 IF(US.LE.15.) GO TO 13

 STOP

 END

 REAL FUNCTION F*8(U)

 REAL*8 U

 COMMON EUF

 F=DSQRT(EUF*(DEXP(-U)+U-1.)+(DEXP(U)-U-1.)/EUF)

 RETURN

 END

 REAL FUNCTION AI*8(U2,U1)

 REAL*8 AI0,U2,U1,DU

 REAL LD

 COMMON EUF /LIST1/ LD

 AI0=1./F(U1)-1./F(U2)

 DU=(U2-U1)/40

 U=U1

 DU 1 I=1,20

 U=U+DU

 AI0=AI0+4./F(U)

 U=U+DU

 AI0=AI0+2./F(U)

 1 CONTINUE

 AI=DABS(LD*(AI0*DU/3.))

 RETURN

 END

```

SUBROUTINE FILL(A,U,K)
COMPLEX A(6,6),JWCK,JWC,CMPLX
COMMON EUF /LIST2/ QP,QN,JWCK,JWC

```

```
P=EUF/EXP(U)
```

```
DO 5 I=1,6
```

```
DO 5 J=1,6
```

```
A(I,J)=CMPLX(0.0,0.0)
```

```
5 CONTINUE
```

```
A(1,4)=CMPLX(QP/P,0.0)
```

```
A(2,5)=CMPLX(QN*P,0.0)
```

```
A(3,6)=JWCK
```

```
A(4,1)=-JWC*P
```

```
A(4,3)=-A(4,1)
```

```
A(5,2)=-JWC/P
```

```
A(5,3)=-A(5,2)
```

```
A(6,1)=A(4,3)
```

```
A(6,2)=A(5,3)
```

```
A(6,3)=A(4,1)+A(5,2)
```

```
RETURN
```

```
END
```

```
SUBROUTINE PC(Y,A1,A2,DX)
```

```
REAL*8 DX
```

```
COMPLEX A1(6,6),A2(6,6)
```

```
COMPLEX*16 Y(6),A1Y(6),A2YP(6),YP(6)
```

```
DO 1 I=1,6
```

```
A1Y(I)=CMPLX(0.0,0.0)
```

```
DO 1 J=1,6
```

```
A1Y(I)=A1Y(I)+A1(I,J)*Y(J)
```

```
1 CONTINUE
```

```
DO 2 I=1,6
```

```
YP(I)=Y(I)-DX*A1Y(I)
```

```
2 CONTINUE
```

```
DO 3 I=1,6
```

```
A2YP(I)=CMPLX(0.0,0.0)
```

```
DO 3 J=1,6
```

```
A2YP(I)=A2YP(I)+A2(I,J)*YP(J)
```

```
3 CONTINUE
```

```
DO 4 I=1,6
```

```
Y(I)=Y(I)-DX*((A1Y(I)+A2YP(I))/2.)
```

```
4 CONTINUE
```

```
RETURN
```

```
END
```

```
SUBROUTINE ORTHN(Z,Y1,Y2)
```

```
COMPLEX*16 Z(6),Y1(6),Y2(6)
```

```
COMPLEX*16 Y12,Y22,Z2,Y1Y2,ZY1,ZY2,CY1,CY2,CZ
```

```
Y12=CMPLX(0.0,0.0)
```

```
DO 1 I=1,6
```

```
Y12=Y12+Y1(I)*Y1(I)
```

```
1 CONTINUE
```

```
CY1=CDSQRT(Y12)
```

```
DO 2 I=1,6
```

```
Y1(I)=Y1(I)/CY1
```

```
2 CONTINUE
```

```
Y1Y2=CMPLX(0.0,0.0)
```

```
DO 3 I=1,6
Y1Y2=Y1Y2+Y1(I)*Y2(I)
3 CONTINUE
DO 4 I=1,6
Y2(I)= Y2(I)-Y1Y2*Y1(I)
4 CONTINUE
Y22=CMPLX(0.0,0.0)
DO 5 I=1,6
Y22=Y22+Y2(I)*Y2(I)
5 CONTINUE
CY2=CDSQRT(Y22)
DO 6 I=1,6
Y2(I)=Y2(I)/CY2
6 CONTINUE
ZY1=CMPLX(0.0,0.0)
ZY2=CMPLX(0.0,0.0)
DO 7 I=1,6
ZY1=ZY1+Z(I)*Y1(I)
ZY2=ZY2+Z(I)*Y2(I)
7 CONTINUE
DO 8 I=1,6
Z(I)=Z(I)-ZY1*Y1(I)-ZY2*Y2(I)
8 CONTINUE
Z2=CMPLX(0.0,0.0)
DO 9 I=1,6
Z2=Z2+Z(I)*Z(I)
9 CONTINUE
CZ=CDSQRT(Z2)
DO 10 I=1,6
Z(I)=Z(I)/CZ
10 CONTINUE
RETURN
END
```

APPENDIX B

CHARGE ANALYSIS PROGRAMS

The low-frequency charge-analysis program uses equations (14) and (17) to produce C-V points. Equations (15) and (16) are used for the high-frequency program. The intergration needed in (16) is performed by subprogram AI using Simpson's rule. These programs can be used for an n-type semiconductor by using negative values for U_F .

INSULATOR CHARACTERISTICS

END OF SUB

SEMICONDUCTOR AND INSULATOR CHARACTERISTICS

NEPS=0.0100E10

KPM=70.0

KNS=10.0

KSM=1.0

KOT=1.0

DIVISION LEVEL AND OPERATING POINT

U=0.0

U=0.0

GENERATING REQUIRED PARAMETERS

UUF=UUF*U

K10=KOT*U

LD=0.5*(1+KSM+KNS*UUF+KSM*UUF**2+KNS*UUF**3)

CO=KOT*U

RES=1.0/(KSM+KNS*UUF+KSM*UUF**2+KNS*UUF**3)

KSEOLD=KSM*CO/LD

KSEOLD=(KSM+KNS*UUF)/LD

UUF=UUF+RES

11 PARM=UUF*(1+KSM*UUF+KNS*UUF**2+KSM*UUF**3+UUF**4)

12 U=UUF**0.5*(1+KSM*UUF+KNS*UUF**2+KSM*UUF**3+UUF**4)**0.5

13 GO TO 11

STARTING PROGRAM CALCULATIONS

14 CONTINUE

U=U*UUF

IF(U<0.0) GO TO 10

U=U*ABS(U)

VLX*Y=U*(U+KSEOLD*UUF)

U=U*(U+KSEOLD*UUF)**0.5*(1+KSM*UUF+KNS*UUF**2+KSM*UUF**3+UUF**4)**0.5

GO TO 2

2 U=KSEOLD*SQRT(UUF*(1+KSM*UUF+KNS*UUF**2+KSM*UUF**3+UUF**4))

```

C THIS PROGRAM GENERATES LOW FREQUENCY C-V POINTS FOR
C GERMANIUM USING CHARGE ANALYSIS
C -----
C REAL NI,K,KO,KS,LD,MN,MP,KTQ,KSEOLD,KSXOLD
C F(U)=SQRT(EUF*(EXP(-U)+U-1.)+(EXP(U)-U-1.)/EUF)
C
C PHYSICAL CONSTANTS AND TEMPERATURE
C
C Q=1.60219E-19
C K=1.38062E-23
C EO=8.8542E-14
C T=296.
C
C INSULATOR THICKNESS
C
C XO=1.E-5
C
C SEMICONDUCTOR AND INSULATOR CONSTANTS
C
C NI=1.8595E13
C MP=1900.
C MN=3900.
C KS=16.
C KO=8.
C
C DOPING LEVEL AND OPERATING POINT
C
C UF=3.
C US=-9.
C
C GENERATING REQUIRED PARAMETERS
C
C EUF=EXP(UF)
C KTQ=K*T/Q
C LD=SQRT((KS*EO*K*T)/(2.*(Q**2)*NI))
C CO=KO*EO/XO
C RES=1./(Q*NI*(MP*EUF+MN/EUF))
C KSEOLD=KS*EO/LD
C KSXOLD=(KS*XO)/(KO*LD)
C WRITE(6,11) UF,RES
11 FORMAT(1H1,///,13X,'LOW FREQUENCY , UF=',F5.2,
1' , RESISTIVITY(OHM-CM)=' ,F10.6///20X,' C/CO
2 VG')
C
C STARTING PROGRAM CALCULATIONS
C
13 CONTINUE
EUS=EXP(US)
IF(US.EQ.0.0) GO TO 1
SUS=US/ABS(US)
VG=KTQ*(US+SUS*KSXOLD*F(US))
CS=SUS*KSEOLD*(EUF*(1.-1./EUS)+(EUS-1.)/EUF)/(2.*F(US))
GO TO 2
1 CS=KSEOLD*SQRT((EUF+1./EUF)/2.)

```


C THIS PROGRAM GENERATES HIGH FREQUENCY C-V POINTS FOR
 C GERMANIUM USING CHARGE ANALYSIS

C -----
 REAL NI,K,KO,KS,LD,MN,MP,KSEOLD,KSXOLD,KTQ
 REAL*8 US,UF,CS,CSL
 COMMON EUF

C PHYSICAL CONSTANTS AND TEMPERATURE

C Q=1.60219E-19
 C K=1.38062E-23
 C E0=8.8542E-14
 C T=296.

C INSULATOR THICKNESS

C X0=1.E-5

C SEMICONDUCTOR AND INSULATOR CONSTANTS

C NI=1.8595E13
 C MP=1900.
 C MN=3900.
 C KS=16.
 C KO=8.

C DOPING LEVEL AND OPERATING POINT

C UF=3.
 C US=-9.

C GENERATING REQUIRED PARAMETERS

C EUF=DEXP(UF)
 C KTQ=K*T/Q
 C LD=SQRT((KS*E0*K*T)/(2.*(Q**2)*NI))
 C KSEOLD=KS*E0/LD
 C KSXOLD=(KS*X0)/(KO*LD)
 C CU=KO*E0/X0
 C RES=1./(Q*NI*(MP*EUF+MN/EUF))
 C WRITE(6,11) UF,RES

11 FORMAT(1H1,///,13X,'HIGH FREQUENCY C-V POINTS',UF=' ',F5.2,
 1' , RESISTIVITY(OHM-CM)=' ',F10.6,///,20X,' ' C/C0
 2 VG')

C STARTING PROGRAM CALCULATIONS

15 CONTINUE
 C EUS=DEXP(US)
 C IF(US.EQ.0.0) GO TO 3
 C SUS=US/DABS(US)
 C SUF=UF/DABS(UF)
 C VG=SNGL(KTQ*(US+SUS*KSXOLD*F(US)))
 C IF(US.LE.UF) GO TO 1

```

CSL=2.*F(UF)/(SUF*(EUF*(1.-1./EUF)+(EUF-1.)/EUF))
CS=KSEOLD/(AI(US,UF)+CSL)

```

```

GO TO 2

```

```

1 CS=SUS*KSEOLD*(EUF*(1.-1./EUS)+(EUS-1.)/EUF)/(2.*F(US))

```

```

GO TO 2

```

```

3 CS=KSEOLD*SQRT((EUF+1./EUF)/2.)

```

```

VG=0.0

```

```

2 CPCO=SNGL(CS/(CO+CS))

```

```

WRITE(6,17) CPCO,US,VG

```

```

17 FORMAT(IH0,20X,F9.7,8X,F4.0,8X,F9.6)

```

```

US=US+1.

```

```

IF(US.LE.15.) GO TO 13

```

```

STOP

```

```

END

```

```

REAL FUNCTION F*8(U)

```

```

REAL*8 U

```

```

COMMON EUF

```

```

F=DSQRT(EUF*(DEXP(-U)+U-1.)+(DEXP(U)-U-1.)/EUF)

```

```

RETURN

```

```

END

```

```

REAL FUNCTION AI*8(U2,U1)

```

```

REAL*8 AI0,U2,U1,DU

```

```

N=(U2-U1)*40.

```

```

NN=N/2

```

```

AI0=1./F(U1)-1./F(U2)

```

```

DU=(U2-U1)/N

```

```

U=U1

```

```

DO 1 I=1,NN

```

```

U=U+DU

```

```

AI0=AI0+4./F(U)

```

```

U=U+DU

```

```

AI0=AI0+2./F(U)

```

```

1 CONTINUE

```

```

AI=DABS(AI0*DU/3.)

```

```

RETURN

```

```

END

```